



# Differential UVR8 Signal across the Stem Controls UV-B–Induced Inflorescence Phototropism

Lucas Vanhaelewyn,<sup>a</sup> Andrés Viczián,<sup>b</sup> Els Prinsen,<sup>c</sup> Péter Bernula,<sup>b,d</sup> Alejandro Miguel Serrano,<sup>e</sup> Maria Veronica Arana,<sup>f</sup> Carlos L. Ballaré,<sup>g,h</sup> Ferenc Nagy,<sup>b</sup> Dominique Van Der Straeten,<sup>a</sup> and Filip Vandenbussche<sup>a,1</sup>

<sup>a</sup>Laboratory of Functional Plant Biology, Department of Biology, Faculty of Sciences, Ghent University, KL Ledeganckstraat 35, B-9000 Gent, Belgium

<sup>b</sup>Institute of Plant Biology, Biological Research Centre, Temesvári körút 62, H-6726 Szeged, Hungary

<sup>c</sup>Department of Biology, University of Antwerp, Groenenborgerlaan 171, 2020 Antwerp, Belgium

<sup>d</sup>Doctoral School in Biology, Faculty of Science and Informatics, University of Szeged, Szeged, H-6726, Hungary

<sup>e</sup>IADIZA, Av. Ruiz Leal s/n Parque Gral. San Martín, Casilla de Correo 507, Mendoza, 5500, Argentina (CONICET)

<sup>f</sup>Instituto de Investigaciones Forestales y Agropecuarias Bariloche, (CONICET-INTA), Modesta Victoria 4450, San Carlos de Bariloche Rio Negro R8403DVZ, Argentina

<sup>g</sup>IFEVA Universidad de Buenos Aires, Av. San Martín 4453, C1417DSE, Buenos Aires, Argentina

<sup>h</sup>IIBIO-INTECH, Universidad Nacional de San Martín, B1650HMP, Buenos Aires, Argentina

ORCID IDs: 0000-0001-5398-6772 (L.V.); 0000-0003-2055-3430 (A.V.); 0000-0003-4320-1585 (E.P.); 0000-0002-5295-5568 (P.B.); 0000-0002-6048-4583 (A.M.S.); 0000-0002-9483-7906 (M.V.A.); 0000-0001-9129-4531 (C.L.B.); 0000-0002-6157-9269 (F.N.); 0000-0002-7755-1420 (D.V.D.S.); 0000-0003-2520-8337 (F.V.)

**In the course of evolution, plants have developed mechanisms that orient their organs toward the incoming light. At the seedling stage, positive phototropism is mainly regulated by phototropin photoreceptors in blue and UV wavelengths. Contrasting with this, we report that UV RESISTANCE LOCUS8 (UVR8) serves as the predominant photoreceptor of UV-B–induced phototropic responses in *Arabidopsis* (*Arabidopsis thaliana*) inflorescence stems. We examined the molecular mechanisms underlying this response and our findings support the Blaauw theory (Blaauw, 1919), suggesting rapid differential growth through unilateral photomorphogenic growth inhibition. UVR8-dependent UV-B light perception occurs mainly in the epidermis and cortex, but deeper tissues such as endodermis can also contribute. Within stems, a spatial difference of UVR8 signal causes a transcript and protein increase of transcription factors ELONGATED HYPOCOTYL5 (HY5) and its homolog HY5 HOMOLOG at the UV-B–exposed side. The irradiated side shows (1) strong activation of flavonoid synthesis genes and flavonoid accumulation; (2) increased gibberellin (GA)2-oxidase expression, diminished GA1 levels, and accumulation of the DELLA protein REPRESSOR OF GA1; and (3) increased expression of the auxin transport regulator PINOID, contributing to diminished auxin signaling. Together, the data suggest a mechanism of phototropin-independent inflorescence phototropism through multiple, locally UVR8-regulated hormone pathways.**

## INTRODUCTION

Light is among the most important environmental cues that steer plant development from germination to senescence. Plants are able to detect light quality, intensity, and direction with photoreceptors, each triggering suitable biological responses to optimize growth and survival (Chen et al., 2004). *Arabidopsis* (*Arabidopsis thaliana*) has a battery of photoreceptors that together perceive nearly the whole spectral range from the UV-B to the far-red light part of the solar spectrum (Galvão and Fankhauser, 2015), including the only UV-B (280 to 315 nm)–specific photoreceptor known to date, UV RESISTANCE LOCUS8 (UVR8; Rizzini et al., 2011). UVR8 action inhibits hypocotyl elongation,

stimulates photoprotective pigment biosynthesis, entrains the circadian clock, increases UV-B tolerance and survival, strengthens defense responses, and has a role in the regulation of UV-B–induced phototropism in seedlings (Tilbrook et al., 2013; Jenkins, 2017). When exposed to UV-B, UVR8 monomerizes in the cytoplasm and then accumulates in the nucleus, where UV-B is further needed for its activity, hence inducing downstream signaling (Kaiserli and Jenkins, 2007; Yin et al., 2016). Key players of the UVR8-mediated signaling pathway have been discovered, including the E3 ubiquitin ligase CONSTITUTIVE PHOTOMORPHOGENIC1 (COP1) and its target transcription factors ELONGATED HYPOCOTYL5 (HY5) and HY5 HOMOLOG (HYH; Ulm et al., 2004; Brown et al., 2005; Oravec et al., 2006; Favory et al., 2009; Binkert et al., 2014; Yin et al., 2016). The well-established model for UVR8 signaling stipulates that UVR8 prevents interaction of COP1 with HY5, causing diminished breakdown of the latter, leading to the activation of HY5 targets, including HY5 itself (Tilbrook et al., 2013; Jenkins, 2017). Recently, it was also shown that UVR8 can enhance HY5 transcription by binding to WRKY DNA BINDING PROTEIN36 (WRKY36), which prevents HY5

<sup>1</sup> Address correspondence to: filip.vandenbussche@ugent.be.

The author responsible for distribution of materials integral to the findings presented in this article in accordance with the policy described in the Instructions for Authors (www.plantcell.org) is: Filip Vandenbussche (filip.vandenbussche@ugent.be).

www.plantcell.org/cgi/doi/10.1105/tpc.18.00929




## IN A NUTSHELL

**Background:** Many plants can bend and turn towards light; this process is called phototropism. Ultraviolet-B (UV-B) radiation is a natural part of sunlight and, similarly to blue light, it has the capacity to cause bending of young *Arabidopsis* seedlings towards the UV-B source. Earlier studies showed that this mechanism is controlled by specialized, light-absorbing proteins, the so-called photoreceptors. In this case, seedling bending towards UV-B is governed by phototropin photoreceptors, which can also detect blue light, together with the UV-B-specific UVR8 photoreceptor. These photoreceptors control processes that lead to differential accumulation of the plant hormone auxin between the irradiated and shaded sides on the plant, resulting in longer cells at the shaded side. This causes bending toward the light.

**Question:** Although considerable knowledge was available on young seedlings, we did not know much about the phototropism of inflorescence stems in the adult plants. We tested how stems perceive and respond to UV-B by studying *Arabidopsis* plants that lack UVR8 (*uvr8* mutant) using molecular biology and microscopy techniques.

**Findings:** We found that the UV-B induced bending of the stem in the adult plant is mediated by the UVR8 photoreceptor, surprisingly, without significant contribution from phototropins. We have established that UVR8 is more active at the illuminated side of the stem compared to the shaded side. This leads to differential signaling between both stem sides resulting in the accumulation of different levels of key signaling proteins and hormones that locally trigger elongation to a different level and thus bending. We also observed that the different layers of the stem contribute to the bending differently, with the outer layers being dominant. We showed that besides auxin, other plant hormones are also required for stem orientation. Taken together our work revealed the molecular basis of a mechanism that causes flowers to orientate towards a UV-B source.

**Next steps:** We would like to further elaborate on the missing steps of the mechanism that we report in this paper. It is also worth examining the biological role of UV-B-induced reorientation of inflorescence stems by performing outdoor experiments.



transcription without UV-B irradiation (Liang et al., 2018). Thus, UV-B causes stabilization and transcriptional induction of HY5 (Ulm et al., 2004; Oravec et al., 2006; Huang et al., 2013). Typical target genes for HY5 include flavonoid biosynthesis genes, such as *CHALCONE SYNTHASE (CHS)* and *FLAVONOL SYNTHASE (FLS)*, that are upregulated by UV-B light. As a consequence, induction of flavonoid synthesis contributes to the protection of macromolecules against UV-B (Jenkins et al., 2001; Hollósy, 2002; Stracke et al., 2010b; Feher et al., 2011; Binkert et al., 2014).

It is well established that UV-B radiation causes photomorphogenic responses that are often hormone dependent. UVR8 signaling is indeed tightly linked to several signaling pathways, including hormonal cascades (reviewed in Vanhaelewyn et al., 2016a). Auxin is a well-known growth hormone in plants, which triggers cell division and cell elongation and regulates development, and has been suggested to be under the control of UVR8 in seedlings (Hayes et al., 2014; Vandenbussche et al., 2014; Fierro et al., 2015). Auxin is not the only growth hormone that is linked to UVR8. Gibberellins (GAs) are known to be responsible for enhancing germination and flowering, and besides these functions, they also promote growth by deactivating growth inhibitor DELLA proteins (Hauvermale et al., 2012). GA2-oxidases play an essential role in controlling the levels of bioactive GA in *Arabidopsis* by inactivating GA by 2 $\beta$ -hydroxylation. GA2-oxidases are HY5 target genes; thus, UV-B diminishes GA levels and growth through its effects on GA2-oxidases (Ulm et al., 2004; Weller et al., 2009; Hayes et al., 2014).

Positive phototropism is often described as the directional growth of plants toward light, which allows plants to optimize the position of their photosynthetic tissues in accordance with the incoming light (Whippo and Hangarter, 2006; Preuten et al., 2013; Vandenbussche et al., 2014). Moreover, in many species, phototropism contributes to flower position and thus influences

pollination (Serrano et al., 2018) as well as seed number and weight (Stanton and Galen, 1989). The directional growth associated with phototropism is established through decreased growth at the irradiated side and stimulated growth at the shaded side of the stem (Christie and Murphy, 2013). The action spectrum of phototropism was recorded between 280 and 500 nm light, revealing the main contributions of UV-A and blue light (Baskin and Iino, 1987; Christie and Murphy, 2013). UV-A and blue light are perceived by phototropins (Briggs and Christie, 2002), yet these photoreceptors are also able to absorb and respond to UV irradiation of shorter wavelength, including UV-B (Guo et al., 2005), resulting in positive phototropism in seedlings (Figure 1A). However, in etiolated seedlings in the absence of active phototropins, a UV-B-controlled positive phototropic response occurs that is entirely dependent on UVR8 (Vandenbussche et al., 2014; Vanhaelewyn et al., 2016b). The latter needs auxin efflux and functional PINOID (PID; Vandenbussche et al., 2014) but is masked in the wild type by phototropin action (Vanhaelewyn et al., 2016b).

*Arabidopsis* has two phototropins, namely PHOTOTROPIN 1 (PHOT1) and PHOT2, that are highly similar in structure, amino acid sequence, and domain organization (Harada et al., 2003). *Phot1 phot2* seedlings show complete lack of phototropism in blue light (Sakai et al., 2001). Beyond the seedling stage, both phototropins regulate phototropism in inflorescence stems in blue light (Christie, 2007; Kagawa et al., 2009). Examination of heliotropism has led to the suggestion of the involvement of plant hormones in the orientation of sunflower buds (Atamian et al., 2016) and an important role for correct auxin signaling (Sato et al., 2015). These findings suggest some degree of conservation regarding auxin dependence of tropisms at various stages of development.

Although the existence of a light gradient within tissues has been shown previously (Seyfried and Fukshansky, 1983; Day et al., 1993),

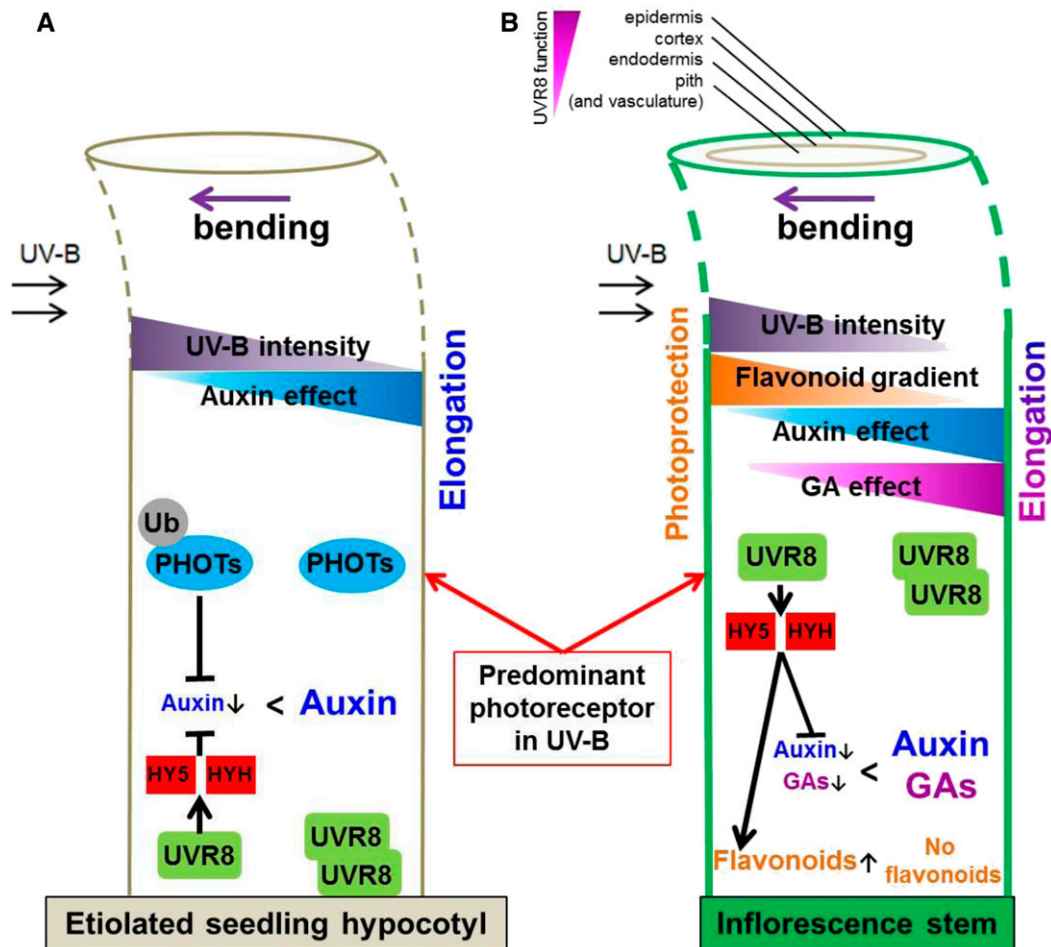


**Figure 1.** Model for Seedling and Inflorescence Stem Bending to Unilateral UV-B light Radiation.

**(A)** Current state of knowledge about UV-B–mediated phototropism. PHOTs are able to absorb and respond to UV-B irradiation and act as the predominant UV-B photoreceptor, resulting in positive phototropism in etiolated seedlings. However, in the absence of active PHOTs, a UV-B–positive phototropic response exists that is UVR8 and HY5/HYH dependent that, in turn, alike PHOTs affects auxin signaling (Eisinger et al., 2003; Christie and Murphy, 2013; Goyal et al., 2013; Briggs, 2014; Vandenbussche et al., 2014; Jenkins, 2017b).

**(B)** Different from seedlings, UVR8 is the dominant UV-B photoreceptor in inflorescence stems. Unilateral exposure to UV-B leads to unilateral UVR8 activation, inducing a strong accumulation of *HY5* and *HYH* transcript and protein. These transcription factors regulate auxin efflux, GA catabolism, and flavonoid biosynthesis. Unilateral UVR8 activity therefore inhibits growth at the irradiated side, whereas the shaded side can still elongate and thus allows bending toward the UV-B source. Arrows next to auxins, GAs, or flavonoids indicate up- or downregulation.

it is only fairly recently that the sites of blue light perception for seedling phototropism have been documented, indicating that PHOT1 expression in the endodermal, cortical, or epidermal cells is sufficient to result in phototropism (Preuten et al., 2013). This highlights the importance of examining tissue-specific subprocesses regarding light signaling cascades. Recent work demonstrates that multiple cell types contribute to UV-B signaling, thus provoking UVR8-mediated inhibition of hypocotyl elongation in seedlings (Bernula et al., 2017; Vanhaelewyn et al., 2019a).

Much of the data in relation with phototropism are obtained from work on hypocotyls of seedlings (Figure 1A). Despite the recent advances in understanding the molecular mechanisms behind the bending of etiolated seedlings toward UV-B (Vandenbussche et al., 2014; Vanhaelewyn et al., 2016b), no reports have been

published about a similar response in inflorescence stems. Here, we investigated the mechanisms of phototropism in response to UV-B radiation in inflorescence stems of adult *Arabidopsis* plants. We find, that in contrast to hypocotyls, UVR8 has a prominent role in the UV-B–mediated phototropism of *Arabidopsis* inflorescences and UV-B, perceived through UVR8, modulates hormone pathways in the irradiated side of the stem, resulting in stem bending toward the UV-B source. By combining physiological experiments performed on a set of *Arabidopsis* mutants with molecular and microscopy techniques, we provide evidence of the action of UV-B on phototropism of inflorescences. We demonstrate that the irradiation with unilateral UV-B triggers differential UVR8 signaling across the stem, with higher signaling state in the epidermis, cortex, and endodermis of the irradiated

side of the stem. In addition, enhanced inhibition of GA biosynthesis and alteration of auxin transport pathways at the irradiated side lead to differential growth, resulting in bending toward the UV-B source (Figure 1B).

## RESULTS

### UVR8-Dependent Bending of the Inflorescence Stem

To investigate UV-B responses in inflorescence stems, we exposed plants in the dark to  $1.3 \mu\text{mol m}^{-2} \text{s}^{-1}$  of unilateral UV-B, hereafter referred to as UV-B treatment, and recorded the stem's position every 15 min by time-lapse photography. Unilateral UV-B treatment caused bending of the wild-type inflorescence stems toward the light source (Figure 2A). The kinetics of the bending indicates that this response starts within an hour after onset of UV-B treatment and appears biphasic, especially visible in the Arabidopsis ecotype Columbia (Col) background, with the first phase being completed in  $\sim 3$  h when plants temporarily move slightly

away from the light source (Figure 2B). Apart from the absence of a biphasic response (quick positive phototropic response, followed by an interruption before bending further), phototropin double mutants (*phot1 phot2*) show a similar phototropic response compared with the wild-type (Col) plants. *Uvr8* mutants display a severely impaired response. When neither phototropins nor UVR8 is functional (*phot1 phot2 amiUVR8*), plants are fully unresponsive to UV-B treatment (Figures 2A and 2B). Hence, UVR8 is the predominant photoreceptor for the phototropic response induced by UV-B light radiation in inflorescence stems.

Because little is known about how UVR8 might control phototropism, we focused on the involvement of the key players of UVR8 signaling (Figure 2C). HY5 and HYH are well established as transcription factors downstream of UVR8 (Brown and Jenkins, 2008); therefore, we tested their involvement in the response. *Hy5* and *hyh* single mutant plants show similar phototropic changes compared with the wild type. By contrast, the double mutant *hy5 hyh* displays a severely reduced bending capacity and rate after the first hour of unilateral UV-B irradiation. After the first hour of bending toward the irradiation, there is a second phase that nearly

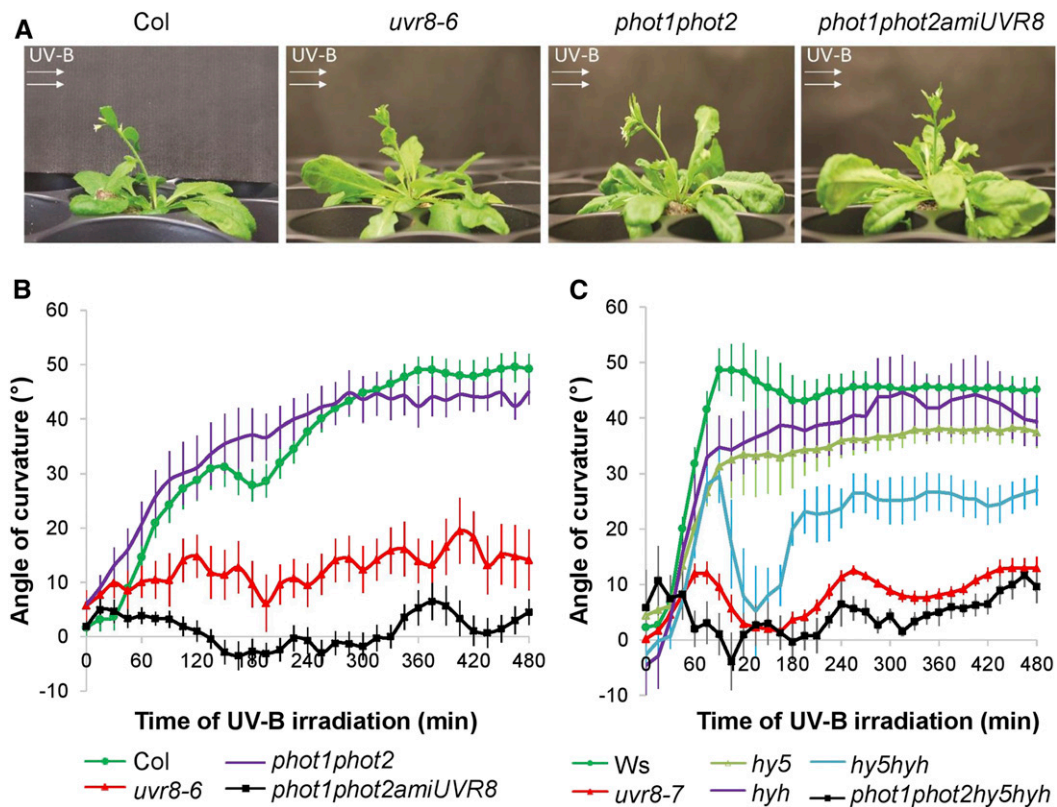


**Figure 2.** Phototropic Response of Arabidopsis Inflorescence Stems under Unilateral UV-B Irradiation.

(A) Photographs of Arabidopsis inflorescence stems having a height of  $\sim 5$  cm that were exposed to unilateral  $1.3 \mu\text{mol m}^{-2} \text{s}^{-1}$  311 nm irradiation for 24 h (UV-B treatment). This UV-B treatment was given to four different genotypes: the wild type (Col), lack-of-function *UVR8* mutant *uvr8-6*, phototropin double mutant *phot1 phot2*, and the triple mutant *phot1 phot2 amiUVR8*. The direction of the UV-B irradiation is indicated by white arrows.

(B) and (C) Kinetic analysis of the phototropic bending response of the inflorescence stems upon UV-B treatment. The bending angle was quantified every 15 min for 8 h. UVR8-deficient lines (*uvr8-6* and *uvr8-7*), phototropin double mutant with or without UVR8 (*phot1 phot2* and *phot1 phot2 amiUVR8*, respectively), *hy5* and *hyh* single and double (*hy5 hyh*) mutants, and a quadruple mutant (*phot1 phot2 hy5 hyh*) are compared with the corresponding wild type (Col and Ws). Error bars indicate SE ( $n \geq 8$ ).

completely reverses the positive phototropic responses that occurred in the first hour. The *phot1 phot2 hy5 hyh* quadruple mutant responds similarly to *phot1 phot2 amiUVR8* (Figures 2B and 2C), suggesting that phototropins do play a role in the bending response but their effect is masked by UVR8 action in the wild type. Moreover, the complete insensitivity to unidirectional UV-B observed in *phot1 phot2 amiUVR8* and *phot1 phot2 hy5 hyh* suggests that there is an interplay between phototropins and

UVR8 photoreceptor pathways, involving a third factor other than HY5 and HYH.

#### Differential Transcript and Protein Levels of UVR8 Signaling Components within Inflorescence Stems

To investigate the spatial characteristics of the mechanisms underlying the UVR8-induced phototropic stem bending, we

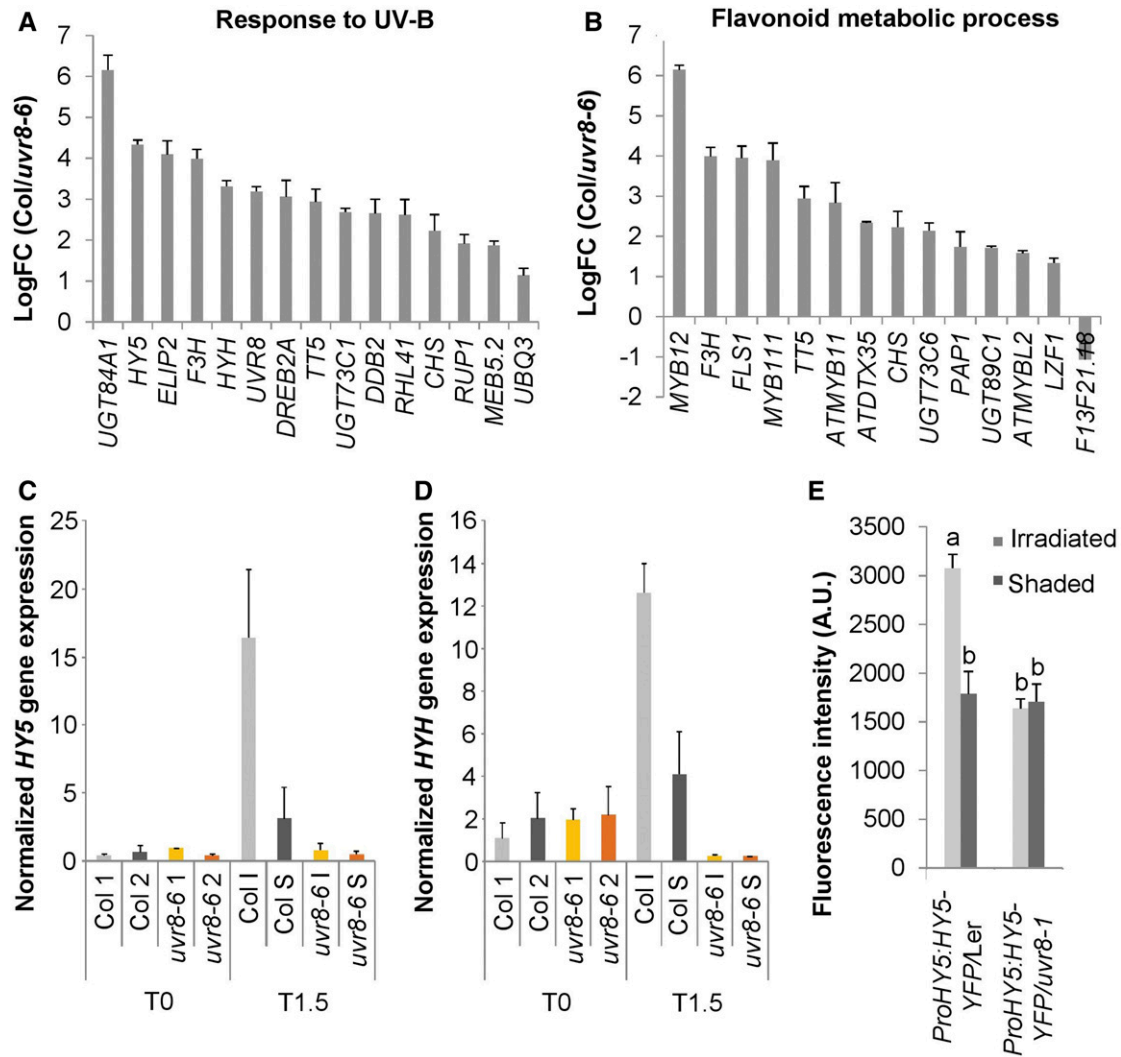


**Figure 3.** Spatial Expression Differences in Arabidopsis Inflorescence Stems Exposed to Unilateral UV-B.

(A) and (B) Gene expression analysis by RNA-seq of the bending zone after 1.5 h of  $1.3 \mu\text{mol m}^{-2} \text{s}^{-1}$  311 nm unilateral UV-B treatment of Col and *uvr8-6* stems. UVR8-regulated genes were selected. Genes with a logFC value higher than 1 and/or lower than  $-1$  with a p-value  $< 0.05$  were selected for GO analysis. The logFC values of the overrepresented genes of the response to UV-B category (A) and the flavonoid metabolic process (B) are shown. With positive values, induced and negative values repressed in Col, compared with *uvr8-6*. Error bars indicate SE ( $n = 3$ ).

(C) and (D) HY5 (C) and HYH (D) expression in inflorescence stems exposed to  $1.3 \mu\text{mol m}^{-2} \text{s}^{-1}$  of unilateral irradiation (UV-B treatment) for 1.5 h (T1.5), or nonexposed inflorescence stems (T0) was determined by RT-qPCR. The irradiated side (I) was dissected from the shaded side (S). Nonexposed plants were dissected longitudinally in two halves without specific positioning (1 and 2), both for the wild type (Col) and *uvr8-6* mutants. Error bars indicate SE ( $n = 3$ ).

(E) Quantification of fluorescent HY5-YFP signal in the inflorescence stem cortex of the wild-type (Ler) or *uvr8-1* plants expressing the ProHY5:HY5-YFP transgene after 3 h of unilateral  $1.3 \mu\text{mol m}^{-2} \text{s}^{-1}$  UV-B treatment. Error bars are SE ( $n \geq 6$ ). The superscript lowercase letters (a, b) indicate statistically significant difference in YFP intensities across the inflorescence stems at the 0.05 level (p-value  $\leq 0.003$ ) based on independent samples Kruskal–Wallis test. A.U., arbitrary units.

developed assays to follow UVR8 signal activity. Transcriptome analysis of the bending zone after 1.5 h of UV-B treatment of the wild type (Col) and *uvr8-6* was conducted using an RNA sequencing (RNA-seq) approach. Among those genes that showed UVR8-specific regulation, we selected genes with a Log fold change (LogFC) value higher than 1 and/or lower than -1 with

p-value < 0.05 for Gene Ontology (GO) analysis (results in Supplemental Data Set 1). The top 20 overrepresented GO categories clearly indicate a response to UV-B and the production of secondary metabolites such as flavonoids and suggest that hormones are involved in UVR8-specific regulation (Figures 3A and 3B; Supplemental Figure 1). The UV-B response GO category

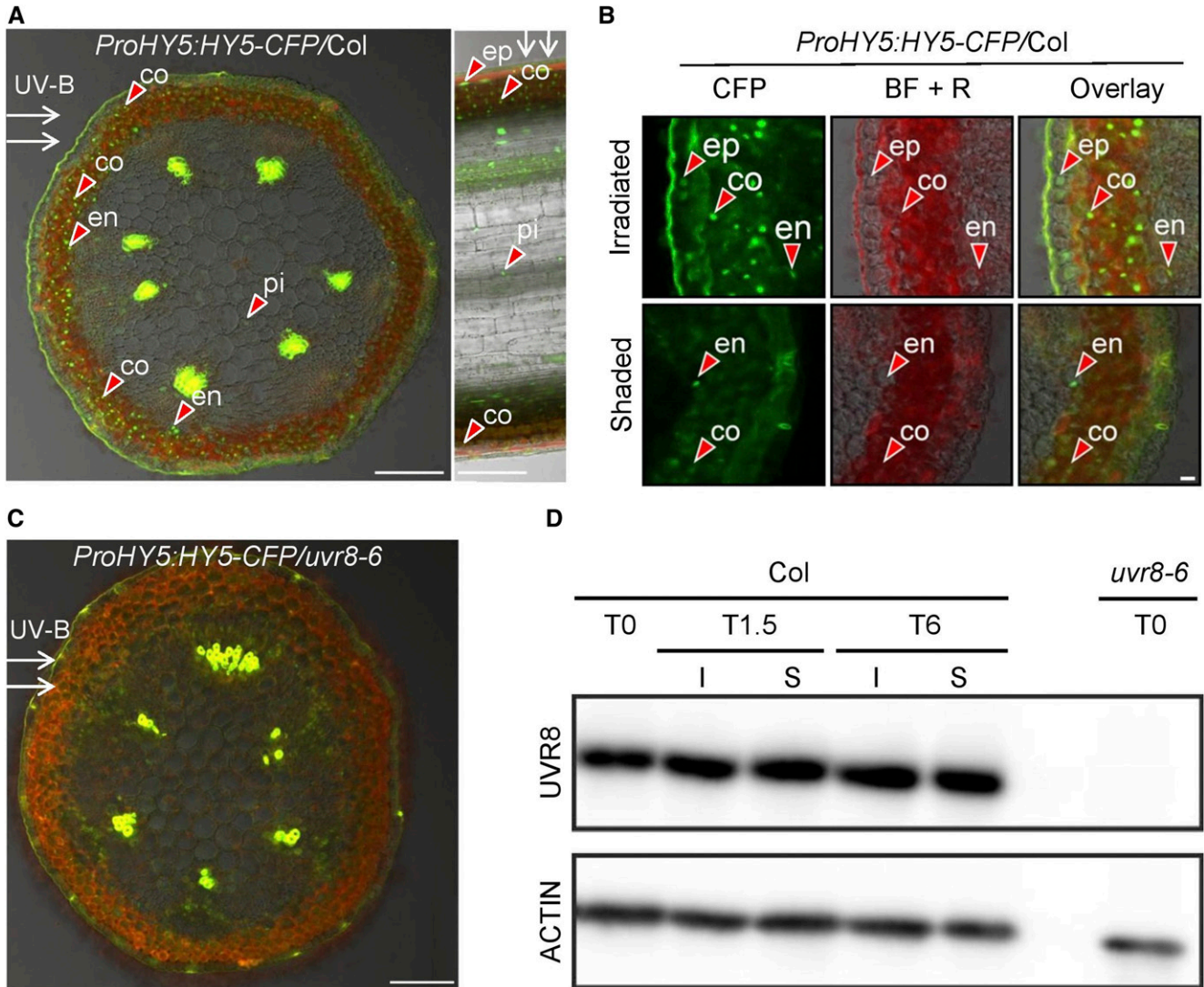


**Figure 4.** Spatial HY5 Protein Accumulation Differences in UV-B-Exposed Arabidopsis Inflorescence Stems.

**(A)** CLSM image of transverse (left) and longitudinal (right) section of a UV-B-treated inflorescence stem taken from a transgenic Col plant expressing the *ProHY5:HY5-CFP* transgene. White arrows indicate the direction of UV-B irradiation; red arrowheads point at selected nuclei containing HY5-CFP signal, observed in the epidermis (ep), cortex (co), endodermis (en), and pith (pi). HY5-CFP accumulation is mainly observed on the irradiated side of the stem. Bar = 100  $\mu$ m.

**(B)** High-resolution CLSM images of transverse section of a UV-B-treated inflorescence stem as described in **(A)**. The CFP channel, bright-field + red channel for autofluorescence (BF + R), and the overlay are displayed from both the irradiated and shaded side. The red arrowheads point at selected nuclei containing HY5-CFP signal. Bar = 10  $\mu$ m.

**(C)** Same as described in **(A)** but using the *uvr8-6* mutant background.

**(D)** Col and *uvr8-6* plants having inflorescence stems of 5-cm height were irradiated with unilateral  $1.3 \mu\text{mol m}^{-2} \text{s}^{-1}$  of UV-B for 1.5 h (T1.5) or 6 h (T6) or were not irradiated (T0). Inflorescence stems were dissected, and total protein extracts were isolated from the shaded (S) and the irradiated (I) stem sides. Immunoblot analysis was used to determine the level of endogenous UVR8 (top), whereas hybridization using ACTIN-specific antibody was applied as loading control (bottom).

included 15 genes, including *ELIP2*, *CHS*, *RUP1*, *HY5*, and *HYH* (Figure 3A).

Because *HY5* and *HYH* are differentially induced in *uvr8* mutants compared with the wild type (Brown and Jenkins, 2008) and we observed phenotypic abnormalities in these loss-of-function mutants (Figure 2C), we examined the expression patterns of these genes in response to unilateral UV-B light. RT-qPCR assays performed on longitudinally separated stems revealed that unilateral UV-B causes *HY5* and *HYH* transcript accumulation on the UV-B-irradiated side compared with the shaded side of the stem and that these responses require functional *UVR8* (Figures 3C and 3D). We also examined the accumulation of HY5 protein using *ProHY5:HY5-YFP*- and *ProHY5:HY5-CFP*-expressing lines. We observed strong nuclear accumulation of HY5-yellow fluorescent protein (YFP) and HY5-cyan fluorescent protein (CFP) proteins on the irradiated side in transverse stem sections in the wild type, but not in *uvr8* background lines (Figures 3E and 4A to 4C; Supplemental Figure 2). Examining the transverse and longitudinal sections using confocal laser scanning microscopy (CLSM; Figures 4A to 4C), we found that HY5-CFP accumulates to a high level in nuclei located in the epidermis, cortex, endodermis, and pith on the irradiated side, but not on the shaded side, of the stem. Similar observations were made using HY5-YFP and HYH-YFP (Supplemental Figures 2 and 3). The observed HY5 and HYH accumulation is dependent on the induced *UVR8* activity on the irradiated side (Figures 4A to 4C), given that unilateral UV-B irradiation does not cause differential *UVR8* protein accumulation in the inflorescence stems (Figure 4D).

GO of our transcriptome analysis indicated a strong enrichment of *UVR8*-dependent regulation of flavonoid synthesis genes, many of which are under *HY5* control (Figure 3B; Sibout et al., 2006). We performed RT-qPCR analysis of *CHS* and *FLS1* and found obvious *UVR8*-dependent upregulation of these flavonoid

biosynthesis genes on the irradiated side of the stem after 1.5 and 6 h of UV-B treatment (Figure 5A; Supplemental Data Set 1). In support of these data, diphenylboric acid 2-aminoethyl ester (DPBA) staining of flavonoids (Stracke et al., 2010a) revealed *UVR8*-dependent flavonoid accumulation, especially in the epidermis and cortex of the irradiated side of those stems that contained functional *UVR8* (Figure 5B). In agreement with the transcriptome data, the *uvr8* mutants globally accumulated less flavonoid in their tissues compared with the wild type, while only minor flavonoid accumulation was observed at the shaded side of the Col, associated with accompanied minor *HY5* accumulation on that side (Figures 4A and 4B).

### UVR8 Expression in Different Cell Types Contributes to Inflorescence Stem Bending

The *UVR8*-induced bending of the inflorescence stem prompted us to investigate to what extent particular cell types in different radial positions within the stem can contribute to UV-B-directed phototropism. To this end, the YFP-*UVR8* chimeric protein was expressed under the control of promoters active in different tissues in the *uvr8-6* mutant background. The endogenous *UVR8* promoter drives expression of the fusion protein (*ProUVR8:YFP-UVR8*) in the epidermis, stomata, cortex, endodermis, and pith (Figures 6A and 6B). Immunoblot analysis showed that the expression level of YFP-*UVR8* in this line is slightly lower than that of endogenous *UVR8* observed in Col (Figure 6C), possibly explaining the somewhat diminished bending response compared with the wild type (Figure 6D). Despite the lack of observable difference of the YFP-*UVR8* level across the stem after UV-B irradiation (Figure 4D), the fusion protein proves to functionally complement the *uvr8-6* mutation (Figure 6D). Interestingly, both *ProML1:YFP-UVR8*, active in the epidermis, and *ProC1:YFP-*

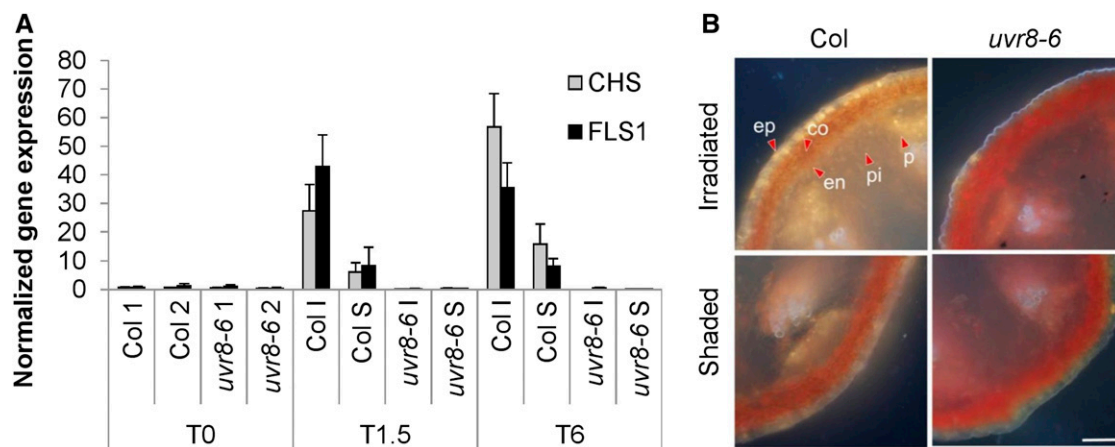


**Figure 5.** Asymmetric Accumulation of Transcripts Encoding Flavonoid Biosynthesis Enzymes and Flavonols.

**(A)** RT-qPCR analysis of *CHS* and *FLS1* gene expression in stems irradiated with unilateral  $1.3 \mu\text{mol m}^{-2} \text{s}^{-1}$  of 311 nm UV-B light for 1.5 h (T1.5) or 6 h (T6) or without UV-B exposure (T0). Irradiated side (I) was dissected from the shaded side (S); stems of nonexposed plants were dissected without orientation in two halves (1 and 2), both for the wild type (Col) and *uvr8-6* mutants. Error bars are  $\text{SE}$  ( $n = 3$ ).

**(B)** Comparison of flavonol content of the irradiated side versus the shaded side of Arabidopsis inflorescence stems after UV-B treatment for 12 h. Transverse sections were made and mounted in DPBA and were documented by epifluorescence microscopy. The quercetin derivatives are visible as yellow/orange; red shows autofluorescence. Arrowheads indicate chosen cells in the epidermis (ep), cortex (co), endodermis (en), phloem (P), and pith (pi). Bar = 100  $\mu\text{m}$ .

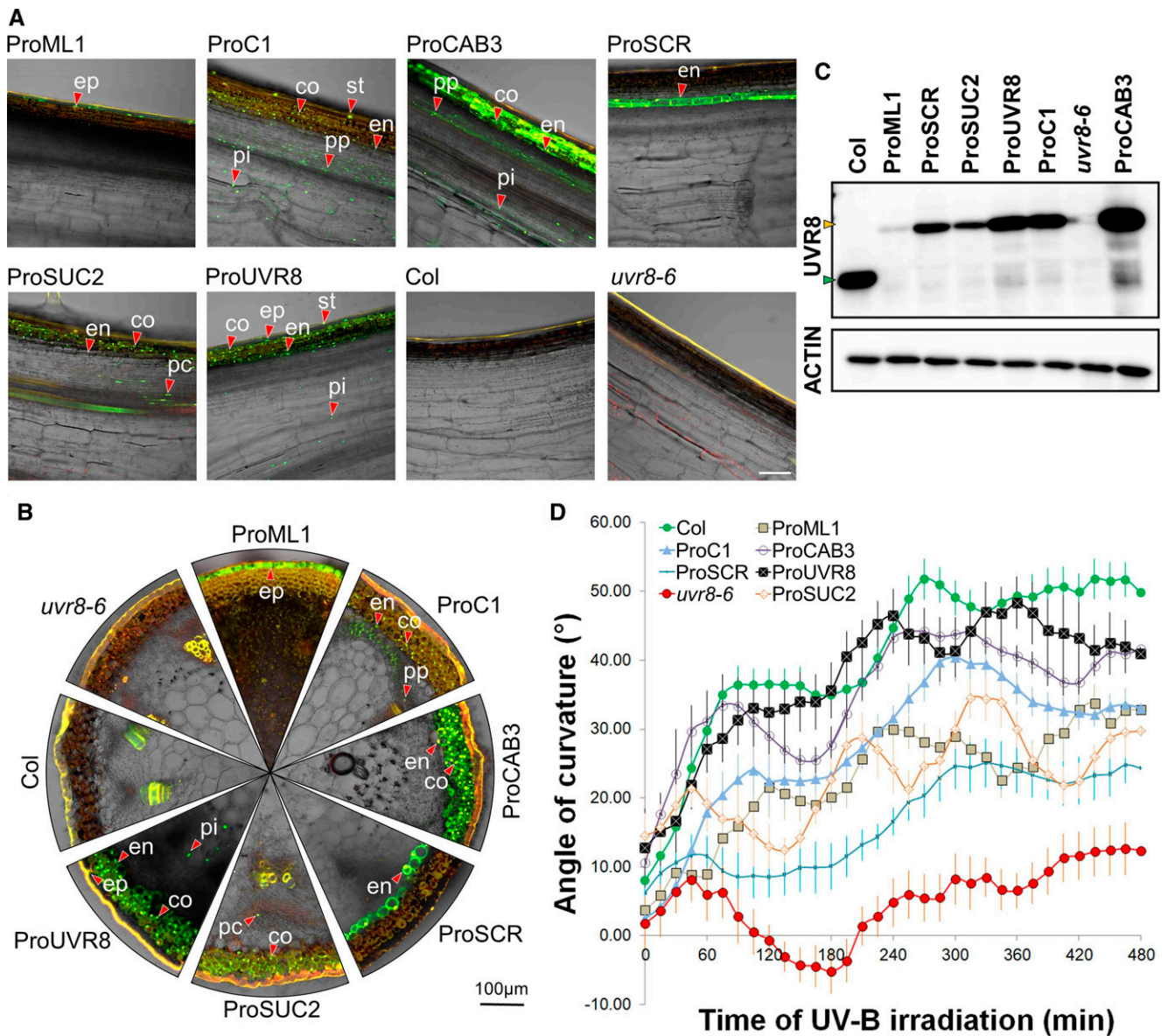


**Figure 6.** Stem Bending Phenotype of the *uvr8* Mutant Can Be Complemented in YFP-UVR8 Expression in Different Cell Types.

**(A)** Longitudinal sections made from Arabidopsis inflorescence stems demonstrate the expression pattern of YFP-UVR8 expressed under the control of different promoters in the *uvr8-6* background. Col and *uvr8-6* are presented as controls. The presented images are the overlay of the green and bright-field channels obtained from CLSM. Green color indicates the YFP signal; red color shows autofluorescence. A few representative nuclei containing YFP-UVR8 are marked in the epidermis (ep), stomata (st), cortex (co), endodermis (en), phloem parenchyma (pp), phloem companion cells (pc), and pith (pi). Bar = 100  $\mu$ m.

**(B)** Transverse sections of the same stems as depicted in (A). The marked nuclei in different tissues are named also as in (A).

**(C)** Immunoblot analysis of UVR8 and YFP-UVR8 expression levels in the inflorescence stems. (Top) Result of the membrane hybridization using the anti-UVR8 antibody, with the green arrowhead indicating native UVR8 and the orange arrowhead indicating YFP-UVR8. (Bottom) Result of immune staining using anti-ACTIN antibody, demonstrating the equal total protein amounts in the lanes.

**(D)** Kinetic analysis of the bending response of Arabidopsis inflorescence stems exposed to unilateral UV-B treatment. Inflorescence stem reorientation was quantified over time. Error bars show  $\pm$  SE ( $n \geq 8$ ). The full names of the transgenic lines throughout this figure are as follows: ProML1, *ProML1:YFP-UVR8/uvr8-6*; ProC1, *ProC1:YFP-UVR8/uvr8-6*; ProCAB3, *ProCAB3:YFP-UVR8/uvr8-6*; ProSCR, *ProSCR:YFP-UVR8/uvr8-6*; ProUVR8, *ProUVR8:YFP-UVR8/uvr8-6*; ProSUC2, *ProSUC2:YFP-UVR8/uvr8-6*.



*UVR8*, active in the cortex, endodermis, and pith (Figures 6A and 6B), complement the mutant to a similar extent (Figure 6D), although the two sets of plants have different YFP-*UVR8* expression levels (Figure 6C). In addition, *ProCAB3:YFP-UVR8*, which is active in the cortex, endodermis, phloem parenchyma, and pith (Figures 6A and 6C), displays a phototropic curvature profile most similar to that of the wild type (Figure 6D). Its YFP-*UVR8* protein expression levels are indeed similar to what is observed in the wild type and higher than in the *ProC1:YFP-UVR8* line (Figure 6C). The response of these lines indicates that both the epidermis and deeper layers contribute to UV-B perception for phototropism. Interestingly, when *UVR8* is solely expressed in the endodermis (*ProSCR:YFP-UVR8*), bending was still restored, yet highly diminished and without a clear biphasic character (Figure 6D). Assuming tight control of transgene expression, the data show that the epidermis, cortex, and endodermis can all serve as UV-B perception sites for stimulating an *UVR8*-mediated phototropic bending response.

Evaluation of the flavonoid accumulation in *ProUVR8:YFP-UVR8* (Supplemental Figure 4) and the wild type (Figure 5B) also designates the epidermis and cortex as main sites of flavonoid accumulation. Interestingly, we see clear flavonoid accumulation in the endodermis of the irradiated side of the *ProSCR:YFP-UVR8* line (Supplemental Figure 4), indicating that flavonoids are induced in the tissue and cell type where *UVR8* is active. Moreover, this, in addition to the *HY5* expression as a marker for the *UVR8* signal (Figures 3C, 4A and 4B), indicates that UV-B light reaches those deeper endodermal cells. We also evaluated the response of the *ProSUC2:YFP-UVR8* line that, apart from the expected accumulation of the fusion protein in phloem companion cells, also expressed YFP-*UVR8* in the outer layers of the cortex, with patchy expression in the endodermis (Figures 6A and 6B). Both in terms of flavonoid accumulation and phototropic bending, this line complemented the mutant phenotype to some extent (Figure 6D; Supplemental Figure 4).

### GA Activity Gradients Are Associated with UV-B-Induced Phototropic Responses

GA inactivation by GA2-oxidases has been suggested to be a target for *UVR8* signaling in seedlings (Hayes et al., 2014). We investigated whether the elongation-controlling hormone GA is involved in the inflorescence stem phototropic response. Our transcriptome data (Supplemental Data Set 1) indicate a strong *UVR8*-dependent induction of *GA2OX1* and *GA2OX8* transcripts 1.5 h after the onset of UV-B treatment. This observation was strengthened by the measurement of the transcript levels by RT-qPCR showing increased accumulation of *GA2OX1* and *GA2OX8* mRNAs on the UV-B-irradiated side of those stems, which contained functional *UVR8* (Figures 7A and 7B). Enhanced *GA2OX* may contribute to decreased GA levels. Therefore, we determined the GA concentration in longitudinally split stems and observed a reduced amount of bioactive GA1 on the irradiated side compared with the shaded side of the bending region (Figure 7C; Supplemental Figure 5B).

Additionally, the nuclear accumulation of the DELLA protein REPRESSOR OF GA1-3 (RGA; Achard et al., 2007) was evaluated in the transverse sections of stems expressing *ProRGA:GFP-*

*RGA*, as an indicator of GA signaling. We clearly detected green fluorescent protein (GFP)-RGA presence in the cortex and endodermis predominantly on the irradiated side (Figures 7D and 7E). This can be caused by a combination of protein stabilization due to GA catabolism by the *GA2OX1* and *GA2OX8* enzymes and direct transcriptional activation of the gene by *HY5* (Lee et al., 2007).

Subsequently, we tested whether the presence of GA is important for UV-B-induced phototropic bending in the wild-type inflorescence stems. We made use of a split stem base assay in which two sides of the inflorescence stem are treated with a different compound to allow for differential inactivation or activation of the GA pathway within the stem under UV-B treatment (Figure 7F). Basal application of the GA biosynthesis inhibitor paclobutrazol (PAC) at both sides of the stem almost completely impairs the bending ability of inflorescence stems toward UV-B, suggesting that GAs are necessary for the response. Moreover, when GA3 is applied at both sides of the stem, the bending is visible, but is less than when PAC is administered at the irradiated side and GA3 at the shaded side. Notably, an artificial GA gradient alone in the absence of unidirectional UV-B, as obtained by applying PAC on one side and GA3 on the other side does not yield bending. These data suggest that differential GA levels, with low levels at the irradiated side, enhance UV-B-induced phototropism, but without unilateral irradiation stimulus, is insufficient to cause bending. Thus, an additional phototropism-associated signal is required for differential growth.

### Differential Auxin Signaling Is Required for Normal UV-B-Induced Phototropic Responses

A wide range of differential growth responses are regulated by auxin (Leyser, 2018). Therefore, we also investigated auxin's involvement in the UV-B-induced stem bending through the use of the synthetic auxin response reporters *ProDR5rev:GFP* (Benková et al., 2003) and *ProDR5rev:3xVenus-N7* (Friml et al., 2003). These reporters revealed a decrease in auxin signaling on the irradiated side of the stems (Figures 8A and 8B; Supplemental Table 1), suggesting that auxin is involved in the phototropic response. Next, we examined the involvement in inflorescence bending of auxin signaling components that are essential for tropisms in seedlings, using seedling tropism defective mutants. Analysis of the dominant gain-of-function mutant *msg2/iaa19* and the double loss-of-function mutant *arf7 arf19* revealed that the functions of *INDOLE-3-ACETIC ACID INDUCIBLE19* (*IAA19*), *AUXIN RESPONSE FACTOR7* (*ARF7*), and *ARF19* are most likely dispensable for UV-B-mediated inflorescence stem phototropism. Only the dominant mutant of *IAA7* (*AUXIN RESISTANT2*, *axr2-1*) was unresponsive, illustrating the necessity of auxin signaling for the response, yet with possible redundancy among *ARFs* (Supplemental Figure 6A).

Tropisms frequently rely on auxin transport. The apical meristem is often regarded as an auxin source. Removing the meristem by decapitation was not sufficient to prevent UV-B phototropism from occurring. However, these plants had a response that lacks a biphasic character (Supplemental Figure 6B). Furthermore, we examined the role of auxin transport in the UV-B phototropic response by auxin transporter mutant analysis and again revealed elimination of the biphasic character of the response by lack of

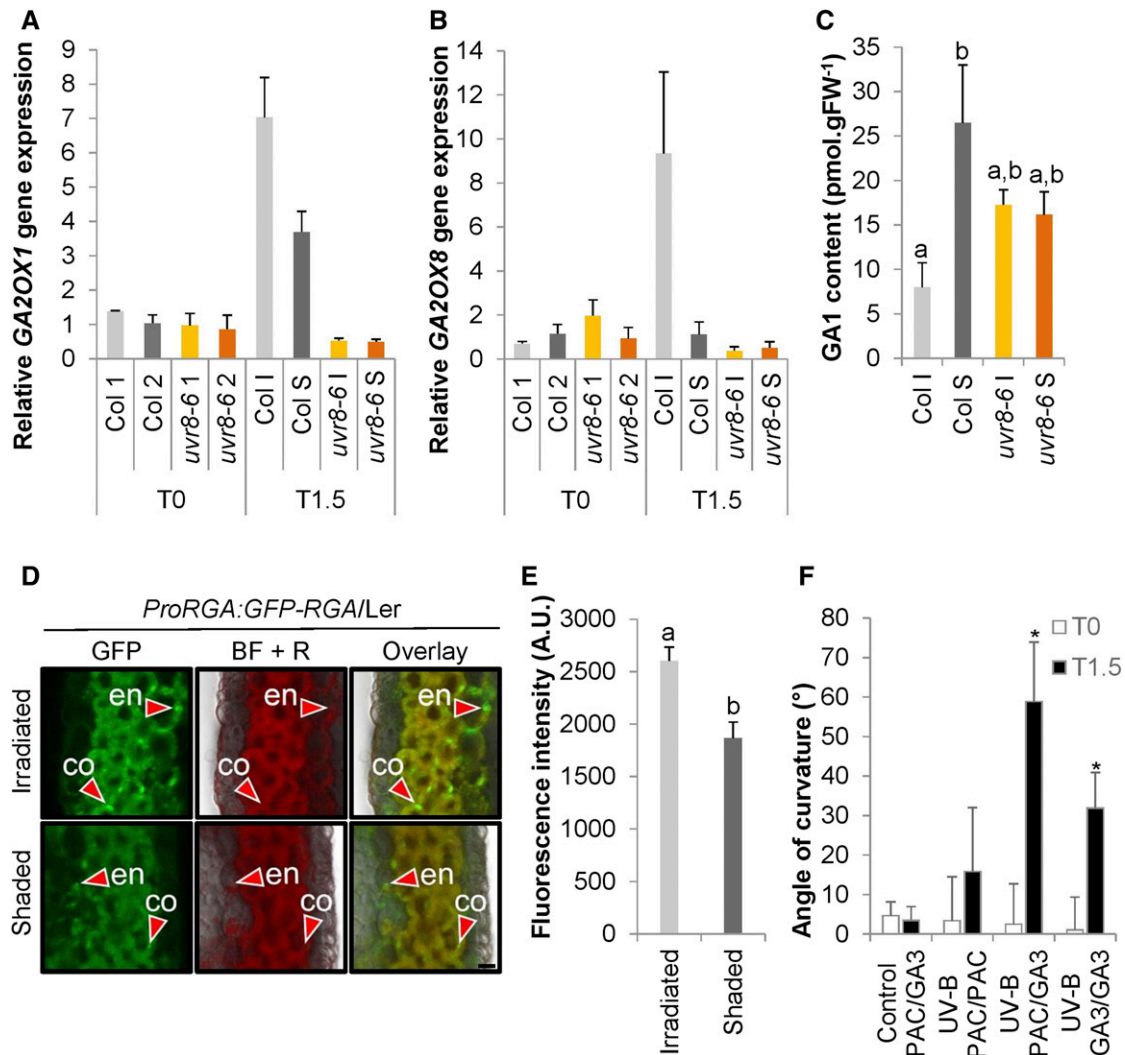


**Figure 7.** Differential GA Signal Is Involved in UV-B-Induced Phototropic Responses.

**(A)** and **(B)** *GA2OX1* **(A)** and *GA2OX8* **(B)** expression was determined in stems that were exposed to  $1.3 \mu\text{mol m}^{-2} \text{s}^{-1}$  of unilateral UV-B irradiation for 1.5 h (T1.5) or nonexposed (T0). The irradiated side (I) was dissected from the shaded side (S), and nonexposed plants were dissected longitudinally without specific direction in two halves (1 and 2), both for the wild type (Col) and *uvr8-6* mutants. Error bars are  $\text{SE}$  ( $n = 3$ ).

**(C)** GA1 content measured in stems after 3 h of UV-B treatment as described in **(A)** and **(B)**. Error bars are  $\text{SE}$  ( $n = 4$ ). The superscript lowercase letters (a, b) indicate statistically significant difference in the GA1 content at the 0.1 level ( $p$ -value = 0.084) based on an independent samples Kruskal–Wallis test.

**(D)** Transverse section of stems from *pRGA:GFP-RGA/Ler* plants after 4 h of UV-B treatment was examined using CLSM. A few representative nuclei containing GFP-RGA are marked with red arrowheads in the cortex (co) and endodermis (en); the GFP channel, bright-field + red channel for autofluorescence (BF + R), and the overlay are displayed from both the irradiated and shaded side. Bar = 10  $\mu\text{m}$ .

**(E)** Quantification of the RGA-GFP signal obtained by CLSM in the stem endodermis of *pRGA:RGA-GFP/Ler* plants irradiated by unilateral UV-B. Error bars indicate  $\text{SE}$  ( $n = 12$ ). The superscript lowercase letters (a, b) indicate statistically significant difference in GFP intensities across the inflorescence stems at the 0.05 level ( $p$ -value = 0.001) based on an independent samples Mann–Whitney U test. A.U., arbitrary units.

**(F)** Angle of curvature of the wild-type (Col) inflorescence stems with a split stem base that had PAC or GA treatment on either side and were subsequently irradiated with unilateral UV-B (UV-B) or kept in white light (control). The measurement of stem curvature was done at the beginning (T0) and after 1.5 h of irradiation (T1.5). Error bars indicate  $\text{SE}$  ( $n \geq 7$ ). The asterisks indicate statistically significant difference in the angle of curvature of inflorescence stems at T1.5 versus T0 at the 0.05 level ( $p$ -value < 0.001) based on a Mann–Whitney U test.

carrier-mediated auxin influx in *aux1 lax1 lax2 lax3* mutants, but no overall reduction in bending (Supplemental Figure 6C). However, when the wild-type stems were pretreated with the auxin efflux inhibitor 1-*N*-naphthylphthalamic acid (NPA), bending disappeared,

indicating a role for auxin efflux (Supplemental Figure 6D). We therefore scanned our transcriptome data for potential HY5 targets relating to auxin efflux (Supplemental Data Set 1) and found that 1.5 h of UV-B treatment triggers the UVR8-dependent upregulation of *PID*,

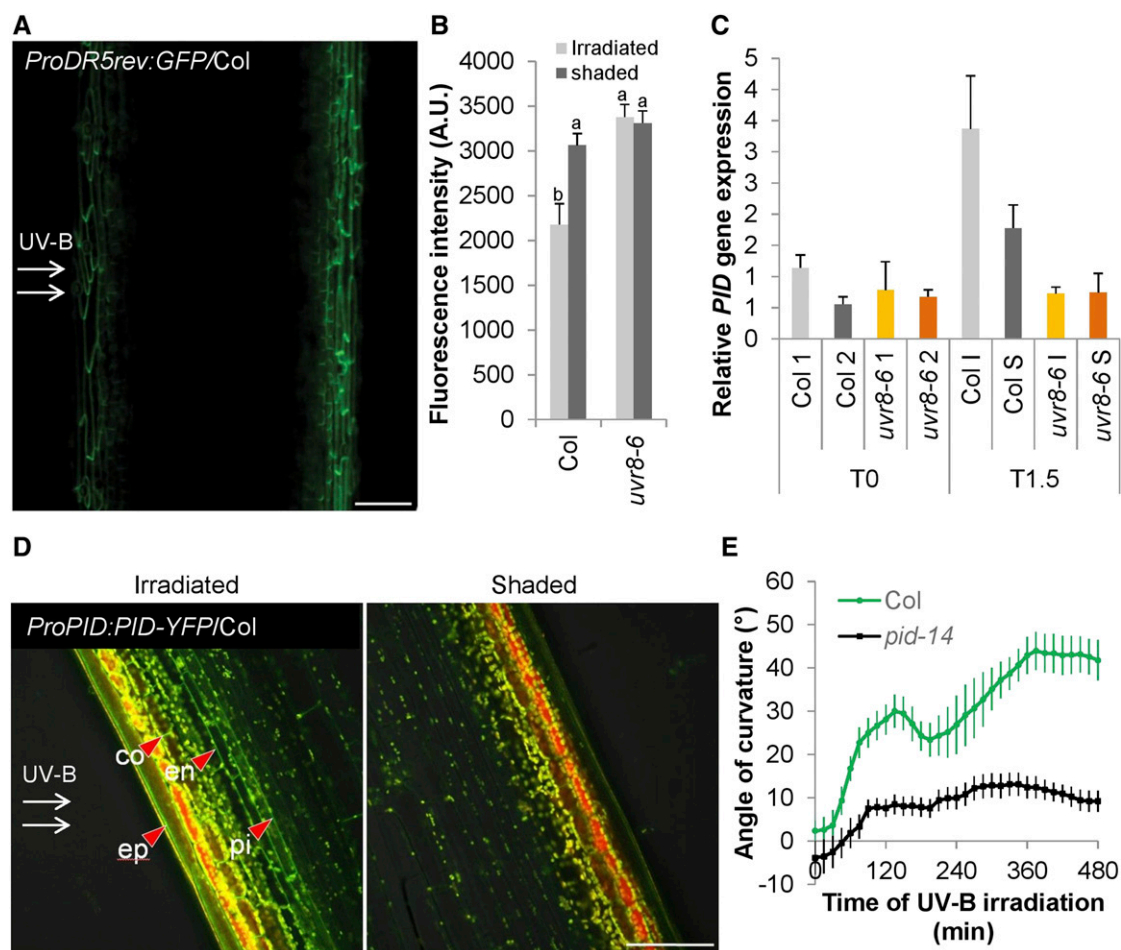


**Figure 8.** Auxin Gradient Is Established for UV-B-Induced Phototropic Responses.

(A) CLSM image of expressing *ProDR5rev:GFP/Col* after 4 h of unilateral  $1.3 \mu\text{mol m}^{-2} \text{s}^{-1}$  UV-B (UV-B treatment). Green color indicates GFP. Bar = 100  $\mu\text{m}$ . (B) Quantification of *ProDR5rev:3xVenus-N7* in the epidermis after 4 h of UV-B treatment based on CLSM. Error bars indicate SE ( $n \geq 9$ ). The superscript lowercase letters (a, b) indicate statistically significant difference in Venus-N7-intensities across the inflorescence stems at the 0.1 level ( $p$ -value = 0.002) based on independent samples Kruskal–Wallis test. A.U., arbitrary units.

(C) RT-qPCR experiment of the *PID* gene expression in stems that were exposed to unilateral UV-B treatment for 1.5 h (T1.5) or nonexposed (T0). The irradiated side (I) was dissected from the shaded side (S), and nonexposed plants were dissected longitudinally without specific direction in two halves (1 and 2), both for the wild type (Col) and *uvr8-6* mutants. Error bars are SE ( $n = 3$ ).

(D) CLSM image of *ProPID:PID-YFP/Col* after 4 h of unilateral UV-B treatment expressed in Col stem. YFP signal is observed in the membranes of the epidermis (ep), cortex (co), endodermis (en), and pith (pi). Green color indicates the YFP signal; yellow and red show autofluorescence. Bar = 100  $\mu\text{m}$ .

(E) Kinetic analysis of the bending response of the UV-B-treated wild-type (Col) and *pid-14* mutant inflorescence stems. Stem orientation was quantified over time. Error bars indicate SE ( $n \geq 12$ ).

a stimulator of auxin efflux (Lee and Cho, 2006; Zourelidou et al., 2014). As *PID* is a potential HY5 target (Lee et al., 2007), we tested the *PID* transcript accumulation and found high levels at the irradiated side in the wild type, but not in the *uvr8* mutant (Figure 8C). We observed a similar pattern in the UV-B-induced *PID*-YFP accumulation in the plasma membranes of inflorescence stem cells of *ProPID:PID-YFP/Col* plants (Figure 8D). Moreover, the *pid-14* mutant shows a significantly reduced bending response to unilateral UV-B radiation, which is similar to that of *uvr8* plants (Figures 2B, 2C, and 8E). Together, these data suggest an active role for *PID* downstream of *UVR8* and *HY5* in regulating UV-B-induced phototropism.

## DISCUSSION

### Different Molecular Mechanisms Involved in the Phototropism of Seedlings and Inflorescence Stems

Phototropism in plants is required for optimization of photosynthesis and also helps many species to increase pollination efficiency and reproductive success (Serrano et al., 2018). For several decades phototropic responses have been well documented, especially concerning the influence of blue light photoreceptors (Liscum and Briggs, 1995, 1996; Kagawa et al., 2001). Blue light-induced phototropic responses are regulated by the action

of phototropins in stem-like organs such as the hypocotyls, petioles, and inflorescence stems (Kagawa et al., 2009).

Our previous study showed that phototropins, which previously were considered to be active in blue light, are the predominant UV-B photoreceptors responsible for phototropic movements of the seedling hypocotyl (Figure 1A; Vandenbussche et al., 2014). Because of practical ease of use, most of the phototropism-related experiments have been performed on etiolated seedlings, including those using UV-B light (Vanhaelewyn et al., 2016b). In this study, we discovered that the data obtained from hypocotyl studies cannot be fully extrapolated to the more complex plant organs such as inflorescence stems. Also, the difference between etiolated tissue and lack of PAR radiation in the seedling assays versus green tissue and presence of PAR radiation in stems may contribute to the differences in UV-B responses.

An important difference between the phototropism of seedlings and inflorescence stems is the importance of HY5 in the response. In seedlings, HY5 alone is required for UV-B-mediated phototropism (Vandenbussche et al., 2014), whereas in inflorescence stems, we found redundancy with HYH (Figure 2C). Both HY5 and HYH share the differential distribution pattern, with high levels at the irradiated side of stems and very low levels at the shaded side of stems (Figures 1B, 3C to 3E, and 4A and 4B; Supplemental Figures 2 and 3). The unilateral differential accumulation of photomorphogenesis-promoting transcription factors such as HY5 and HYH fits in the model proposed by Blaauw (1919), who states that during phototropism differential growth is caused by unilateral inhibition of growth, thereby explaining at least part of the bending response observed here. Such expression differences are indicative of a signal gradient that is established within the plant and may be caused by different light penetration and could therefore be less pronounced in etiolated seedlings than in inflorescence stems. We found that this gradient is visible at different levels of the UVR8 signaling pathway, ranging from the induction of *HY5/HYH* to the accompanied accumulation of flavonoids, and it is in good agreement with previous findings (Sibout et al., 2006). Moreover, since HY5 and HYH also work downstream of photoreceptors that perceive wavelengths longer than UV-B wavelength, similar mechanisms to drive phenotypic outputs may be expected at other wavelengths. This will of course depend on the optical properties of the tissues, and differential responses may be less pronounced for UV-B light, which penetrates less deeply into plant tissues compared with longer wavelengths (Markstädter et al., 2001; Qi et al., 2003).

### UV-B Signaling Occurs Locally

Our data suggest that unilateral  $1.3 \mu\text{mol m}^{-2} \text{s}^{-1}$  UV-B irradiation can reach the endodermis and pith of the stem, thus reaching radial cell layers of different identity where the UVR8 signal leads to flavonoid accumulation (Figure 5B). Moreover, the UVR8-dependent flavonoid accumulation appears to be controlled in a tissue-autonomous manner (Supplemental Figure 4). These results indicate that flavonoid synthesis happens locally, where UV-B light was perceived, and that the transport of flavonoids between tissues, as described between the shoot and the root (Buer et al., 2007), is not particularly important across the inflorescence stems. Similar observations were recently reported

about UV-B-induced flavonoid accumulation in the cotyledons and hypocotyls of young seedlings (Bernula et al., 2017; Vanhaelewyn et al., 2019a). When it comes to regulation of growth upon perception of a specific signal, some cell layers can be more important than others (Savaldi-Goldstein et al., 2007). Along with this finding, it is worth noting the exceptional effectiveness of the small amount of epidermal UVR8 (*ProML1:YFP-UVR8*) in driving a considerable bending response (Figures 6C and 6D), indicating the privileged role of the epidermis in UV-B sensing and signaling. This is in good agreement with the UVR8-dependent photomorphogenic responses found in seedlings (Bernula et al., 2017; Vanhaelewyn et al., 2019a). However, the best complementation of the *uvr8* mutation for bending was seen in those lines where UVR8 was expressed at high levels in the cortex cells. Along with this finding, we noted that both HY5 and HYH accumulate in the epidermis and cortex cells upon UVR8 activation (Figures 4A and 4B; Supplemental Figures 2 and 3); thus, it is tempting to link these cell types with the bending response redundantly controlled by these factors (Figure 2C). To fully complement the mutant phenotype, significant contributions of epidermal and endodermal expression of *UVR8* are also necessary.

### UV-B Signaling Connects to Auxin Transport Machinery

The decreased signal observed in *ProDR5rev*-based synthetic auxin response reporters and the accumulation of PINOID auxin efflux transporter (Lee and Cho, 2006; Zourelidou et al., 2014) at the irradiated side of the stem and PINOID's key role in the bending itself, underline the role of auxin transport for tropic growth (Figure 8). These results suggest the importance of the PID/WAG-mediated repolarization of PIN proteins, which was already shown to be essential for phototropic responses (Ding et al., 2011). In hypocotyls, PIN3 polarity is aligned with the direction of the light stimulus and probably directs the auxin flow toward the shaded side, where auxin induces growth and thus a bending response of the hypocotyls toward the light (Ding et al., 2011). Although PIN3 together with PIN7 appear as primary auxin transporters in inflorescence stems (Bennett et al., 2016), their involvement in UV-B-stimulated inflorescence phototropism remains to be seen. Furthermore, another class of proteins comprising auxin efflux regulators, the ABCB transporters, deserves particular attention in this phototropic response, since they are targets for flavonol control (Bouchard et al., 2006; Bailly et al., 2008). Flavonoids were shown to inhibit auxin transport in inflorescence stems, hypocotyls, and roots and to influence tropisms (Brown et al., 2001; Peer and Murphy, 2007; Lewis et al., 2011). For example, asymmetric distribution of flavonoids modulates asymmetric auxin transport and drives root gravitropism (Santelia et al., 2008) and root phototropism (Silva-Navas et al., 2016). It is therefore tempting to speculate that the unilateral accumulation of flavonoids at the illuminated side of the inflorescence stems may cause a unilateral block in auxin transport, thus further contributing to the bending response.

Mobile signals such as hormones are transported to the responding cells from distant tissues to initiate phototropic growth responses. The apical meristem is often referred to as an excellent source of auxin; hence, it is not surprising that decapitated inflorescence stems have slower kinetics of bending than intact

stems, including the lack of a biphasic character of the response (Supplemental Figure 6B). It is even more interesting that decapitated stems still bend well toward UV-B, suggesting that the apex as auxin source in the short term is dispensable for inflorescence phototropism, and the majority of the response may be controlled in the bending stem tissue itself. The biphasic character in the wild-type Col-0 in the presence of an intact meristem and auxin transport machinery (Figure 8E; Supplemental Figure 6) suggests pulsed auxin flow from the meristem into the stem during the response, contributing to a quicker response. At this point, we do not know whether this is an overlap with nutations coinciding with stem growth (Britz and Galston, 1983). We also noted the different bending characteristics of Col and Wassilewskija (Ws) ecotypes, the latter of which shows no biphasic curve. We speculate that this phenomenon is the result of differences in auxin levels between the two ecotypes, which could be caused by the phytochrome D deficiency of Ws (Aukerman et al., 1997). Phytochromes have already been found to affect the kinetics of the inflorescence bending toward blue light (Kumar and Kiss, 2006), but their contribution to phototropism in UV-B requires further investigation.

### Concerted Hormonal Action Leads to Stem Bending under UV-B Irradiation

While auxins have been shown to operate mainly in the epidermis of the root, the situation in the shoot is less clear, even though also here the epidermis has been suggested as determining tissue for auxin-driven growth (Procko et al., 2016). The latter was also indirectly confirmed by recent work that maps the site of ethylene action as a fine-tuner of auxin-induced growth to the epidermis of both root and shoot (Vaseva et al., 2018). In contrast to auxins, GAs are believed to exert their effect on growth in the endodermis (Ubeda-Tomás et al., 2009; Shani et al., 2013). The UVR8-dependent upregulation of the GA signal inhibiting DELLA proteins at the irradiated side in endodermis and cortex (Figure 7D) overlaps with this zone of activity and may therefore indicate a direct control of growth by light. Both UVR8-regulated *GA2OX1* and *GA2OX8* are likely direct HY5 targets (Lee et al., 2007). Therefore, HY5 (redundantly with HYH) may function on one hand by inhibiting the GA signal through upregulation of *GA2OX1* and *GA2OX8* (Figure 7; Supplemental Data Set 1) and on the other hand by depleting intracellular auxin by increasing the expression of *PID* (Figures 8C and 8D). In addition, HY5 is known to promote the expression of negative regulators of auxin signaling, which is consistent with HY5 acting as a signaling hub linking light and hormone signaling (Cluis et al., 2004). The bending assays also indicate that the less studied homolog of HY5, HYH, may function similarly under UV-B (Figure 2C). Although both auxins and GAs are established growth stimulators, only auxin appears to limit the differential regulation of growth. The UVR8 control of hormone-regulated phototropism thus appears to differ mechanistically from that of the phototropins, which depend mainly on lateral auxin distribution (Ding et al., 2011). Depending on the fate of auxin upon leaving the cells at the irradiated side in a PID-dependent manner, our data may also support the model of Went (1926) and Cholodny (1927), stipulating that phototropic bending is caused by the lateral distribution of the growth hormone auxin. If

this is the case, then both the Blaauw and the Cholodny–Went models could be unified in the inflorescence stem. All of our data are summarized in a model in Figure 1B.

### Functional Aspects of Hypocotyl and Stem Bending

These observations indicate a stark contrast between the UV-B–induced photomorphogenesis of inflorescence stems (Figure 1B) and seedling hypocotyls (Vandenbussche et al., 2014). Whereas the contribution of phototropins dominates the response of the hypocotyl bending, their role in the stem bending of adult plants is almost negligible and UVR8 primarily governs the response to UV-B. From a mechanistic viewpoint, this response is not controlled by changes in gene expression of the photoreceptors, as the level of *UVR8*, *PHOT1*, and *PHOT2* expression remains rather constant during the plant's life cycle (Supplemental Figure 7; Schmid et al., 2005; Winter et al., 2007). Instead, changes in the function of these proteins during the plant's life cycle may be ecologically significant. Thus, early in the plant's life cycle, phototropins direct etiolated seedlings in their search of light for photosynthesis through phototropic curvature, leaf positioning, leaf flattening, stomatal opening, and chloroplast relocation (Inoue et al., 2010). Inflorescence stems, however, are parts of a usually well-established photosynthetically active plant and have reproduction as an additional key function. UV-B radiation is a light signal that can help plants to locate gaps in the canopy and increase their exposure to sunlight (Mazza and Ballaré, 2015). Increased exposure is often discussed in the context of light capture and photosynthesis but can also be important to maximize flower visibility and to increase inflorescence temperature, which are important factors in the context of plant–pollinator interactions (Serrano et al., 2018). UV-B irradiation is also known to induce the synthesis of floral volatiles to attract specific pollinators in some species (Falara et al., 2013; Amarasinghe et al., 2015) and flavonoid-derived pigments that are determinants of flower color (Khoo et al., 2017; Serrano et al., 2018). Hence, if the phenomenon of inflorescence phototropism that we have described in *Arabidopsis* is common in other species, UV-B radiation could be an important environmental factor regulating inflorescence development and plant reproductive success in patchy canopies.

### METHODS

#### Plant Materials, Molecular Cloning, and Generation in Transgenic Plants

We used the following genotypes of *Arabidopsis thaliana* in the study: *uvr8-6* (Favory et al., 2009), *phot1-5 phot2-1* (Kinoshita et al., 2001), *phot1 phot2 amiUVR8* (Vandenbussche et al., 2014), *aux1lax1-lax2lax3* (Bainbridge et al., 2008), *nph4arf19* (Okushima et al., 2005), *msg2-1* (Tatematsu et al., 2004), *axr2-1* (Timpote et al., 1994), *ProDR5rev:GFP/Col* (Benková et al., 2003), *ProDR5rev:3xVenus-N7/Col* (Friml et al., 2003), and *pid-14* (Huang et al., 2010) were in Col-0 ecotype, whereas the *hy5-KS50*, *hyh*, *hy5 hyh* (Holm et al., 2002), and *uvr8-7* (Favory et al., 2009) mutants are in Ws ecotype. *Phot1 phot2 hy5 hyh* was isolated from the F3 of a cross between *phot1 phot2* and *hy5 hyh*. The *ProHY5:HY5-YFP/hy5* (in Landsberg *erecta* [Ler] background; Oravec et al., 2006), was a kind gift of Roman Ulm, whereas *ProHY5:HY5-YFP/uvr8-1* was obtained by crossing. *GFP* in the *ProHY5:HY5-GFP pPCV812* vector (Kirchenbauer et al., 2016)

was exchanged to the CFP coding region (*SmaI*-*SacI* fragment), resulting in the *ProHY5:HY5-CFP pPCV812* binary vector, which was used to transform Col and *uvr8-6* lines. *ProHY5:HY5-CFP pPCV812* was then used to introduce the promoter and coding region of *HYH* (*HindIII*-*BamHI* and *BamHI*-*SmaI* fragment, respectively), resulting in the *ProHYH:HYH-YFP pPCVB* binary vector, which we used to transform Col and *uvr8-6* lines. The *ProML1:YFP-UVR8/uvr8-6*, *ProCAB3:YFP-UVR8/uvr8-6*, *ProSUC2:YFP-UVR8/uvr8-6*, and *ProUVR8:YFP-UVR8/uvr8-6* were described previously by Bernula et al. (2017). The *ProC1:YFP-UVR8* and *ProSCR:YFP-UVR8* constructs were made in the following way: Gateway compatible primers with attB sites adjoining the YFP-UVR8 fragment (Bernula et al., 2017) were amplified in a Phusion High-Fidelity DNA Polymerase (Thermo Fisher Scientific – Life Technologies) PCR reaction. BP reaction was performed according to the standard Invitrogen protocol with a pDONR201 vector (Thermo Fisher Scientific – Life Technologies). The *C1* (AT1G09750) and the *SCR* (AT3G54220) promoters were provided as *pENTRP4-P1R-ProC1* (Preuten et al., 2013) and *pENTRP4-P1R-ProSCR* (Abbas et al., 2018) vectors and were both a kind gift from Miguel Blázquez (Valencia, Spain). LR reaction was performed according to the standard Invitrogen protocol. Plants were transformed with the *pH7m24GW-ProSCR:YFP-UVR8* and *pH7m24GW-ProC1:YFP-UVR8* binary vectors using the floral dip method (Clough and Bent, 1998). We raised 15 to 20 independent transgenic lines containing each construct and selected those that segregated regarding the transgene as a single Mendelian trait. We studied at least three independent lines with similar results.

### General Growth Conditions

For the bending assays, plants were initially sown on Jiffy peat pellets (Intergrow NV), initially supplemented with 1:500 Wuxal Super N8-P8-K6 N,P,K (OptimAgro). Constant growth conditions of 22°C and 70% humidity in 16-h-light/8-h-dark light cycles using 65  $\mu\text{mol m}^{-2} \text{s}^{-1}$  of white light in a white-walled Weiss WK21' growth chamber (Weiss Technik) were maintained during the vegetative and early flowering stage of the plants.

### Kinetics of Bending

Four hours after dawn, plants having a primary inflorescence stem of 5 to 7 cm in height were transferred to a growth room with black walls providing a constant temperature of 22°C. Inflorescence stems were exposed to unilateral 311 nm UV-B from a TL01 lamp (Philips) filtered through two layers of cellulose acetate film (Jürgen Rachow) for UV-B treatment, to remove all radiation below 295 nm, yielding 1.3  $\mu\text{mol m}^{-2} \text{s}^{-1}$  (0.5  $\text{W m}^{-2}$ ) of UV-B light. Plants were photographed every 15 min by a webcam-based time-lapse photography system with focal plane parallel with the incoming unilateral UV-B (Vandenbussche et al., 2010; Vanhaelewyn et al., 2019b). The obtained images were analyzed using the angle measurement tool of ImageJ (National Institutes of Health). The angle of curvature is defined as the angle between the upper end of the inflorescence stem and the vertical lower part and can thus be seen as deviation from the vertical, with 0° being vertical, 90° being horizontal and directed toward the light source, and -90° being horizontal and directed away from the light source.

### Sectioning and Microscopy

After UV-B treatment, the inflorescence stems were stained with Calcofluor Fluorescent Brightener 28 (Sigma-Aldrich) at the shaded side and left to dry for at least 1 min, using a paint brush before sectioning the plant material. Next, the bending region was excised from the inflorescence with a razor blade and side branches and leaves were removed. Subsequently, a cylindrical transparent support was filled with a liquid 7% low melting point agarose solution (Sigma-Aldrich) and the plant material was quickly embedded in the agarose, which solidifies in less than 10 min. The plant

material was positioned vertically, permitting perpendicular positioning in a vibrating microtome (HM560, Thermo Fisher Scientific – Life Technologies). Sections of 100  $\mu\text{m}$  were cut during all experiments. The sections were analyzed using a confocal laser scanning microscope (EZC1, Nikon), applying the same gain, laser, and pinhole settings (150  $\mu\text{m}$ , 1.2 aperture size), resulting in images containing no saturated pixels and allowing signal comparison between samples. We determined the nuclear fluorescent signal both on the irradiated and shaded sides of the stems, setting the irradiated side of UV-B-treated plants as a reference for maximum signal. GFP or YFP was detected using 488 nm excitation light and a 515 to 530 nm bandpass filter, and CFP was detected with 405 nm excitation light and a 515 to 530 nm bandpass filter. Nuclear signal was quantified in the green channel of at least 10 nuclei for each orientation, allowing to distinguish the nuclear fluorescent signal from autofluorescence (red channel) at both the irradiated and the shaded side of the stem taken from at least 10 individual plants using CLSM Advanced Research analysis software (Nikon). All calculations were done in Microsoft Excel.

### RNA Sequencing

Col and *uvr8-6* Arabidopsis inflorescence stems of 5 to 7 cm in height were harvested, after 1.5 h of unilateral 1.3  $\mu\text{mol m}^{-2} \text{s}^{-1}$  311 nm exposure. The top and the bottom 1 cm of the stems and also the leaves were removed, resulting in a 3-cm-long sample that was promptly frozen in liquid nitrogen. Each sample contained three to four stems originating from different plants. Triplicate sampling was performed, and each of three samples was treated and harvested on different days. Plant tissues were homogenized by the use of a ball mill (Retsch). RNA was extracted with the RNeasy Mini kit according to the manufacturer's instructions with on-column DNase treatments (Qiagen). RNA-seq was performed on poly(A) tailed molecules by VIB Nucleomics Core, with a NextSeq500 platform, using a TruSeq library prep kit (Illumina). Artifact reads (all but three bases in the read equal one base type), poly(A) reads (>90% of the bases equal A), low-quality reads (>50% of the bases <Q25), and ambiguous reads (comprising N) were removed. More than 4 million fragment reads per sample remained after trimming and preprocessing. These fragments were aligned with the Arabidopsis genome in The Arabidopsis Information Resource (TAIR 10.21). Reads from the alignment that are nonprimary mappings or have a mapping quality  $\leq 20$  were removed with Samtools 1.1 (Sourceforge.net). Approximately 94% of the fragments could be mapped after filtering. 14,276 unique sequences were left out for which all samples have less than 1 counts per million (absent genes), leaving 19,326 genes. The GC-content was fixed per sample with the EDASeq package from Bioconductor (Bioconductor.org), allowing full quantile normalization on bins of GC-content. Correction for sample-specific variation was also done with the Bioconductor EDASeq package. Subsequently, a statistical analysis of expression differences was performed on each gene. The resulting p-values were corrected for multiple testing with Benjamini-Hochberg adjustment to control the false discovery rate. Once p-values were computed, all genes with a logFC above or below 1 or -1, respectively with a p-value < 0.05 were selected. The Unique gene identifier (Gene ID), Gene name, logFC (the  $\log_2$ -ratio as calculated by edgeR) and PValue (the p-values of the likelihood ratio test, as calculated by edgeR) are indicated in Supplemental Data Set 1. Negative logFC values have induced gene expression in Col versus *uvr8-6* and vice versa. GO was performed with BiNGO (Maere et al., 2005).

### RT-qPCR Split Stem Experiment

Arabidopsis inflorescence stems were treated and harvested as described under "RNA Sequencing," but the irradiated side and shaded side of the inflorescence stems were separated longitudinally with a scalpel after the UV-B treatment. Each sample consists of a pool of three stems that

received the same light treatment and were promptly frozen in liquid nitrogen. RNA was prepared using Qiagen RNeasy Plant Mini kits (Qiagen), and cDNA was synthesized using the cDNA Verso kit (Thermo Fisher Scientific – Life Technologies) according to the manufacturer's instructions. qRT-PCR was performed using the SyGreen (qPCRBIOS) qPCR kit. Reactions were performed in an iCycler thermal cycler and an iQ5 optical system (Bio-Rad) as optical module for multicolor signal detection. Data were analyzed with QBase software (Biogazelle; Hellemans et al., 2007), where expression values were normalized with reference genes At4G34270, AT4G26410, AT1G18070, and AT1G69960. The relative expression level is automatically calculated in Qbase+. Primer sequences are indicated in Supplemental Table 2.

### In Situ Flavonoids DPBA Staining

Arabidopsis inflorescence stems were exposed to  $1.3 \mu\text{mol m}^{-2} \text{s}^{-1}$  of 311 nm unilateral UV-B for 12 h. Transverse sections were made using a double-bladed platina-coated razor blade. The sections were mounted on microscope slides in DPBA staining solution consisting of an aqueous solution of 0.25% (w/v) DPBA and 0.00375% (v/v) Triton X-100 (Stracke et al., 2010a). After 5 min of staining, the samples were analyzed and photographs were taken using a Rebel camera (Canon) mounted on a Axiovert 200M inverted microscope (Zeiss). Excitation light was provided using a tungsten light source supplied with a 365 nm filter. Emission was detected using a 420 nm long pass filter (Zeiss filterset 02).

### Plant Protein Isolation and Immunoblot Analysis

Parts similar to the 5-cm-high inflorescence stems used for RNA isolation were collected and snap-frozen in liquid nitrogen. The samples were ground using 5-mm glass balls in a Mixer Mill (MM301, Retsch). The subsequent total protein isolation and immunoblot analysis procedures were described previously by Bauer et al. (2004). The applied anti-UVR8 antibody was also used as described previously by Heijde and Ulm (2013). The signal was detected using Immobilon Western Chemiluminescent HRP Substrate (Millipore) according to the manufacturer's instructions. Anti-ACTIN antibody (catalog no. A048, batch no. 054M4805V, Sigma-Aldrich) was used in a dilution of 1:10,000 to check the equal amount of proteins between the different lanes.

### GA Measurements

Samples (~20 mg fresh weight) were MagNaLysed (Roche) and extracted overnight in acidified methanol, pH 4 (80:20, methanol:5 mM formic acid). As internal tracers, d2-GA<sub>1</sub>, d2-GA<sub>4</sub>, d2-GA<sub>8</sub>, d2-GA<sub>9</sub>, d2-GA<sub>15</sub>, d2-GA<sub>19</sub>, d2-GA<sub>20</sub>, and d2-GA<sub>29</sub> (20 pmol each, Olchemim Lth) were added. After purification on a C18 cartridge (500 mg, Varian), samples were derivatized with *N*-(3-dimethylaminopropyl)-*N'*-ethylcarbodiimide (Sigma-Aldrich; 1 mg/sample, at pH 4, 1 h, 37°C under continuous shaking, Eppendorf thermomixer) and analyzed by ultra-performance liquid chromatography–tandem mass spectrometry (ACQUITY, TQD, Waters) using an ACQUITY BEH C18 column (2.1 × 50 mm, 1.7 mm, Waters).

### Pharmacological Treatments

Four hours after dawn, the Col wild-type 5- to 10-cm stems were cut from their rosette and subsequently put in 1.5-mL microcentrifuge tubes containing tap water and the respective biochemical or solvent, so that approximately the basal 1 cm was submerged. For split stem base assays, the stem was sectioned in two equal halves from the base to 1.5-cm height. Each half was submerged to 1 cm from the base into microcentrifuge tubes containing the respective solution (200  $\mu\text{M}$  PAC, 100  $\mu\text{M}$  GA<sub>3</sub>, and 100  $\mu\text{M}$  NPA). Subsequently, stems were exposed to unilateral  $1.3 \mu\text{mol m}^{-2} \text{s}^{-1}$

UV-B or kept in control conditions ( $5 \mu\text{mol m}^{-2} \text{s}^{-1}$  uniform abaxial white light) for 1.5 h. Bending of the stems was followed using time lapse photography and subsequent image analysis in ImageJ. NPA was purchased from Greyhound and PAC and GA<sub>3</sub> were from Sigma-Aldrich.

### Statistical Analysis

Statistical analyses were performed with SPSS 25.0 (IBM SPSS). Data analyses included bivariate nonparametric tests (i.e., independent samples Kruskal–Wallis test and Mann–Whitney U test), with the output detailed in Supplemental Data Set 2.

### Accession Numbers

Sequence data from this article can be found in the GenBank/EMBL data libraries under accession numbers NM\_125781.4 (UVR8), NM\_126218.3 (RGA), NM\_129019.5 (PID), AB005456.1 (HY5), AF453477.1 (HYH), AJ132435.1 (GA2OX1), NM\_118239.3 (GA2OX8).

### Supplemental Data

**Supplemental Figure 1.** Top 20 overrepresented biological process GO categories of UVR8-regulated genes in Arabidopsis inflorescence stems. Supports Figures 3A and 3B.

**Supplemental Figure 2.** HY5-YFP accumulates on the irradiated side of UV-B–exposed Arabidopsis inflorescence stems. Supports Figures 4A and 4B.

**Supplemental Figure 3.** UVR8-dependent HYH induction. Supports Figure 3D.

**Supplemental Figure 4.** Flavonol accumulation in the inflorescence stems of plants expressing YFP-UVR8 in different cell types. Supports Figures 5 and 6B.

**Supplemental Figure 5.** Gibberellin accumulation in UV-B–exposed inflorescence stems. Supports Figure 7C.

**Supplemental Figure 6.** Particular auxin signaling and transport components are important for Arabidopsis inflorescence stem bending. Supports Figure 8.

**Supplemental Figure 7.** Expression levels of *UVR8*, *PHOT1* and *PHOT2* at two stages of plant development under continuous light conditions.

**Supplemental Table 1.** Comparison of the fluorescence intensity ratio of the shaded vs irradiated side of UV-B–exposed inflorescence stems.

**Supplemental Table 2.** Oligonucleotides used in the study.

**Supplemental Data Set 1.** RNaseq transcriptome data set of the bending zone after 1.5 h of UV-B treatment of the wild type (Col) and *uvr8-6*.

**Supplemental Data Set 2.** Output of the statistical analysis from Figures 3E, 7C, 7E, 7F, and 8B.

### ACKNOWLEDGMENTS

This work was supported by the Research Foundation Flanders (FWO) (research project G000515N to F.V. and E.P., as of October 2017 administratively transferred to D.V.D.S.); the FWO-Hungarian Academy of Sciences international collaboration project (VS07416N to F.V. and NKM-45/2016 to A.V.); the FWO-CONICET (Argentina) international collaboration

project (VS00715N to D.V.D.S. and C.L.B.); and Ghent University to D.V.D.S. The work in Hungary was supported by the Economic Development and Innovation Operative Program (grants GINOP-2.3.2-15-2016-00001, GINOP-2.3.2-15-2016-00015, and GINOP-2.3.2-15-2016-00032). L.V. is a predoctoral fellow of the FWO. We thank Christine Yung Hung (Ghent University) for statistical advice, Mary Williams (American Society of Plant Biologists) for constructive comments that helped to improve the article, and Olivier Leroux (Ghent University) for providing insights on plant histology techniques.

#### AUTHOR CONTRIBUTIONS

F.V. conceived the project with contributions of A.V., M.V.A., D.V.D.S., and E.P.. L.V. performed most of the experimental work, some of it with cooperation of F.V. (Figures 2, 3A, 3B, 3E, 4A to 4C, 5B, 6A, 6B, 6D, 7C to 7F, 8A, 8B, 8D and 8E; Supplemental Figures 2 to 5, 6A and 6D). A.V. contributed Figures 4D and 6C and provided support for Figures 4A to 4C and Supplemental Figure 3. E.P. determined plant hormone content (Figure 7C; Supplemental Figure 5), A.M.S. contributed to Supplemental Figure 6C. P.B., L.V., and F.V., contributed to Figures 1 and 3E and provided support for Figure 6C. L.V., F.V., and A.V. wrote the article. D.V.D.S., E.P., P.B., M.V.A., C.L.B., F.N., and A.M.S. commented on the article. All authors contributed to scientific discussion.

Received December 12, 2018; revised May 28, 2019; accepted June 25, 2019; published July 9, 2019.

#### REFERENCES

- Abbas, M., Hernandez-Garcia, J., Pollmann, S., Samodelov, S.L., Kolb, M., Friml, J., Hammes, U.Z., Zurbruggen, M.D., Blázquez, M.A., and Alabadi, D. (2018). Auxin methylation is required for differential growth in *Arabidopsis*. *Proc. Natl. Acad. Sci. USA* **115**: 6864–6869.
- Achard, P., Liao, L., Jiang, C., Desnos, T., Bartlett, J., Fu, X., and Harberd, N.P. (2007). DELLAs contribute to plant photomorphogenesis. *Plant Physiol.* **143**: 1163–1172.
- Amarasinghe, R., Poldy, J., Matsuba, Y., Barrow, R.A., Hemmi, J.M., Pichersky, E., and Peakall, R. (2015). UV-B light contributes directly to the synthesis of chiloglottone floral volatiles. *Ann. Bot.* **115**: 693–703.
- Atamian, H.S., Creux, N.M., Brown, E.A., Garner, A.G., Blackman, B.K., and Harmer, S.L. (2016). Circadian regulation of sunflower heliotropism, floral orientation, and pollinator visits. *Science* **353**: 587–590.
- Aukerman, M.J., Hirschfeld, M., Wester, L., Weaver, M., Clack, T., Amasino, R.M., and Sharrock, R.A. (1997). A deletion in the PHYD gene of the *Arabidopsis* Wassilewskija ecotype defines a role for phytochrome D in red/far-red light sensing. *Plant Cell* **9**: 1317–1326.
- Bailly, A., Sovero, V., Vincenzetti, V., Santelia, D., Bartnik, D., Koenig, B.W., Mancuso, S., Martinoia, E., and Geisler, M. (2008). Modulation of P-glycoproteins by auxin transport inhibitors is mediated by interaction with immunophilins. *J. Biol. Chem.* **283**: 21817–21826.
- Bainbridge, K., Guyomarc'h, S., Bayer, E., Swarup, R., Bennett, M., Mandel, T., and Kuhlemeier, C. (2008). Auxin influx carriers stabilize phyllotactic patterning. *Genes Dev.* **22**: 810–823.
- Baskin, T.I., and Iino, M. (1987). An action spectrum in the blue and ultraviolet for phototropism in alfalfa. *Photochem. Photobiol.* **46**: 127–136.
- Bauer, D., Viczián, A., Kircher, S., Nobis, T., Nitschke, R., Kunkel, T., Panigrahi, K.C., Adám, E., Fejes, E., Schäfer, E., and Nagy, F. (2004). Constitutive photomorphogenesis 1 and multiple photoreceptors control degradation of phytochrome interacting factor 3, a transcription factor required for light signaling in *Arabidopsis*. *Plant Cell* **16**: 1433–1445.
- Benková, E., Michniewicz, M., Sauer, M., Teichmann, T., Seifertová, D., Jürgens, G., and Friml, J. (2003). Local, efflux-dependent auxin gradients as a common module for plant organ formation. *Cell* **115**: 591–602.
- Bennett, T., Hines, G., van Rongen, M., Waldie, T., Sawchuk, M.G., Scarpella, E., Ljung, K., and Leyser, O. (2016). Connective auxin transport in the shoot facilitates communication between shoot apices. *PLoS Biol.* **14**: e1002446.
- Bernula, P., Crocco, C.D., Arongaus, A.B., Ulm, R., Nagy, F., and Viczián, A. (2017). Expression of the UVR8 photoreceptor in different tissues reveals tissue-autonomous features of UV-B signaling. *Plant Cell Environ.* **40**: 1104–1114.
- Binkert, M., Kozma-Bognár, L., Terecskei, K., De Veylder, L., Nagy, F., and Ulm, R. (2014). UV-B-responsive association of the *Arabidopsis* bZIP transcription factor ELONGATED HYPOCOTYL5 with target genes, including its own promoter. *Plant Cell* **26**: 4200–4213.
- Blaauw, A.H. (1919). Licht und Wachstum III. Mededelingen Landbouwhogeschool Wageningen **15**: 89–204.
- Bouchard, R., Bailly, A., Blakeslee, J.J., Oehring, S.C., Vincenzetti, V., Lee, O.R., Paponov, I., Palme, K., Mancuso, S., Murphy, A.S., Schulz, B., and Geisler, M. (2006). Immunophilin-like TWISTED DWARF1 modulates auxin efflux activities of *Arabidopsis* P-glycoproteins. *J. Biol. Chem.* **281**: 30603–30612.
- Briggs, W.R. (2014). Phototropism: Some history, some puzzles, and a look ahead. *Plant Physiol.* **164**: 13–23.
- Briggs, W.R., and Christie, J.M. (2002). Phototropins 1 and 2: Versatile plant blue-light receptors. *Trends Plant Sci.* **7**: 204–210.
- Britz, S.J., and Galston, A.W. (1983). Physiology of movements in the stems of seedling *Pisum sativum* L. cv Alaska: III. Phototropism in relation to gravitropism, nutation, and growth. *Plant Physiol.* **71**: 313–318.
- Brown, B.A., and Jenkins, G.I. (2008). UV-B signaling pathways with different fluence-rate response profiles are distinguished in mature *Arabidopsis* leaf tissue by requirement for UVR8, HY5, and HYH. *Plant Physiol.* **146**: 576–588.
- Brown, B.A., Cloix, C., Jiang, G.H., Kaiserli, E., Herzyk, P., Kliebenstein, D.J., and Jenkins, G.I. (2005). A UV-B-specific signaling component orchestrates plant UV protection. *Proc. Natl. Acad. Sci. USA* **102**: 18225–18230.
- Brown, D.E., Rashotte, A.M., Murphy, A.S., Normanly, J., Tague, B.W., Peer, W.A., Taiz, L., and Muday, G.K. (2001). Flavonoids act as negative regulators of auxin transport in vivo in *Arabidopsis*. *Plant Physiol.* **126**: 524–535.
- Buer, C.S., Muday, G.K., and Djordjevic, M.A. (2007). Flavonoids are differentially taken up and transported long distances in *Arabidopsis*. *Plant Physiol.* **145**: 478–490.
- Chen, M., Chory, J., and Fankhauser, C. (2004). Light signal transduction in higher plants. *Annu. Rev. Genet.* **38**: 87–117.
- Cholodny, N.G. (1927). Wuchshormone und Tropismen bei den Pflanzen. *Biol. Zentralbl.* **47**: 604–626.
- Christie, J.M. (2007). Phototropin blue-light receptors. *Annu. Rev. Plant Biol.* **58**: 21–45.
- Christie, J.M., and Murphy, A.S. (2013). Shoot phototropism in higher plants: New light through old concepts. *Am. J. Bot.* **100**: 35–46.
- Clough, S.J., and Bent, A.F. (1998). Floral dip: A simplified method for *Agrobacterium*-mediated transformation of *Arabidopsis thaliana*. *Plant J.* **16**: 735–743.
- Cluis, C.P., Mouchel, C.F., and Hardtke, C.S. (2004). The *Arabidopsis* transcription factor HY5 integrates light and hormone signaling pathways. *Plant J.* **38**: 332–347.



- Day, T.A., Martin, G., and Vogelmann, T.C. (1993). Penetration of UV-B radiation in foliage: Evidence that the epidermis behaves as a non-uniform filter. *Plant Cell Environ.* **16**: 735–741.
- Ding, Z., Galván-Ampudia, C.S., Demarsy, E., Łangowski, Ł., Kleine-Vehn, J., Fan, Y., Morita, M.T., Tasaka, M., Fankhauser, C., Offringa, R., and Friml, J. (2011). Light-mediated polarization of the PIN3 auxin transporter for the phototropic response in Arabidopsis. *Nat. Cell Biol.* **13**: 447–452.
- Eisinger, W.R., Bogomolni, R.A., and Taiz, L. (2003). Interactions between a blue-green reversible photoreceptor and a separate UV-B receptor in stomatal guard cells. *Am. J. Bot.* **90**: 1560–1566.
- Falara, V., Amarasinghe, R., Poldy, J., Pichersky, E., Barrow, R.A., and Peakall, R. (2013). The production of a key floral volatile is dependent on UV light in a sexually deceptive orchid. *Ann. Bot.* **111**: 21–30.
- Favory, J.J., et al. (2009). Interaction of COP1 and UVR8 regulates UV-B-induced photomorphogenesis and stress acclimation in Arabidopsis. *EMBO J.* **28**: 591–601.
- Feher, B., Kozma-Bognar, L., Kevei, E., Hajdu, A., Binkert, M., Davis, S.J., Schafer, E., Ulm, R., and Nagy, F. (2011). Functional interaction of the circadian clock and UV RESISTANCE LOCUS 8-controlled UV-B signaling pathways in *Arabidopsis thaliana*. *Plant J.* **67**: 37–48.
- Fierro, A.C., Leroux, O., De Coninck, B., Cammue, B.P., Marchal, K., Prinsen, E., Van Der Straeten, D., and Vandebussche, F. (2015). Ultraviolet-B radiation stimulates downward leaf curling in *Arabidopsis thaliana*. *Plant Physiol. Biochem.* **93**: 9–17.
- Friml, J., Vieten, A., Sauer, M., Weijers, D., Schwarz, H., Hamann, T., Offringa, R., and Jürgens, G. (2003). Efflux-dependent auxin gradients establish the apical-basal axis of Arabidopsis. *Nature* **426**: 147–153.
- Galvão, V.C., and Fankhauser, C. (2015). Sensing the light environment in plants: Photoreceptors and early signaling steps. *Curr. Opin. Neurobiol.* **34**: 46–53.
- Goyal, A., Szarzynska, B., and Fankhauser, C. (2013). Phototropism: At the crossroads of light-signaling pathways. *Trends Plant Sci.* **18**: 393–401.
- Guo, H., Kottke, T., Hegemann, P., and Dick, B. (2005). The phot LOV2 domain and its interaction with LOV1. *Biophys. J.* **89**: 402–412.
- Harada, A., Sakai, T., and Okada, K. (2003). Phot1 and phot2 mediate blue light-induced transient increases in cytosolic Ca<sup>2+</sup> differently in Arabidopsis leaves. *Proc. Natl. Acad. Sci. USA* **100**: 8583–8588.
- Hauvermale, A.L., Atrizumi, T., and Steber, C.M. (2012). Gibberellin signaling: A theme and variations on DELLA repression. *Plant Physiol.* **160**: 83–92.
- Hayes, S., Velanis, C.N., Jenkins, G.I., and Franklin, K.A. (2014). UV-B detected by the UVR8 photoreceptor antagonizes auxin signaling and plant shade avoidance. *Proc. Natl. Acad. Sci. USA* **111**: 11894–11899.
- Heijde, M., and Ulm, R. (2013). Reversion of the Arabidopsis UV-B photoreceptor UVR8 to the homodimeric ground state. *Proc. Natl. Acad. Sci. USA* **110**: 1113–1118.
- Hellemans, J., Mortier, G., De Paepe, A., Speleman, F., and Vandesompele, J. (2007). qBase relative quantification framework and software for management and automated analysis of real-time quantitative PCR data. *Genome Biol.* **8**: R19.
- Hollósy, F. (2002). Effects of ultraviolet radiation on plant cells. *Micron* **33**: 179–197.
- Holm, M., Ma, L.G., Qu, L.J., and Deng, X.W. (2002). Two interacting bZIP proteins are direct targets of COP1-mediated control of light-dependent gene expression in Arabidopsis. *Genes Dev.* **16**: 1247–1259.
- Huang, F., Zago, M.K., Abas, L., van Marion, A., Galván-Ampudia, C.S., and Offringa, R. (2010). Phosphorylation of conserved PIN motifs directs Arabidopsis PIN1 polarity and auxin transport. *Plant Cell* **22**: 1129–1142.
- Huang, X., Ouyang, X., Yang, P., Lau, O.S., Chen, L., Wei, N., and Deng, X.W. (2013). Conversion from CUL4-based COP1-SPA E3 apparatus to UVR8-COP1-SPA complexes underlies a distinct biochemical function of COP1 under UV-B. *Proc. Natl. Acad. Sci. USA* **110**: 16669–16674.
- Inoue, S., Takemiya, A., and Shimazaki, K. (2010). Phototropin signaling and stomatal opening as a model case. *Curr. Opin. Plant Biol.* **13**: 587–593.
- Jenkins, G.I. (2017). Photomorphogenic responses to ultraviolet-B light. *Plant Cell Environ.* **40**: 2544–2557.
- Jenkins, G.I., Long, J.C., Wade, H.K., Shenton, M.R., and Bibikova, T.N. (2001). UV and blue light signalling: Pathways regulating chalcone synthase gene expression in Arabidopsis. *New Phytol.* **151**: 121–131.
- Kagawa, T., Sakai, T., Suetsugu, N., Oikawa, K., Ishiguro, S., Kato, T., Tabata, S., Okada, K., and Wada, M. (2001). Arabidopsis NPL1: A phototropin homolog controlling the chloroplast high-light avoidance response. *Science* **291**: 2138–2141.
- Kagawa, T., Kimura, M., and Wada, M. (2009). Blue light-induced phototropism of inflorescence stems and petioles is mediated by phototropin family members phot1 and phot2. *Plant Cell Physiol.* **50**: 1774–1785.
- Kaiserli, E., and Jenkins, G.I. (2007). UV-B promotes rapid nuclear translocation of the Arabidopsis UV-B specific signaling component UVR8 and activates its function in the nucleus. *Plant Cell* **19**: 2662–2673.
- Kho, H.E., Azlan, A., Tang, S.T., and Lim, S.M. (2017). Anthocyanidins and anthocyanins: Colored pigments as food, pharmaceutical ingredients, and the potential health benefits. *Food Nutr. Res.* **61**: 1361779.
- Kinoshita, T., Doi, M., Suetsugu, N., Kagawa, T., Wada, M., and Shimazaki, K. (2001). Phot1 and phot2 mediate blue light regulation of stomatal opening. *Nature* **414**: 656–660.
- Kirchenbauer, D., Viczián, A., Ádám, É., Hegedűs, Z., Klose, C., Leppert, M., Hiltbrunner, A., Kircher, S., Schäfer, E., and Nagy, F. (2016). Characterization of photomorphogenic responses and signaling cascades controlled by phytochrome-A expressed in different tissues. *New Phytol.* **211**: 584–598.
- Kumar, P., and Kiss, J.Z. (2006). Modulation of phototropism by phytochrome E and attenuation of gravitropism by phytochromes B and E in inflorescence stems. *Physiol. Plant.* **127**: 304–311.
- Lee, S.H., and Cho, H.T. (2006). PINOID positively regulates auxin efflux in Arabidopsis root hair cells and tobacco cells. *Plant Cell* **18**: 1604–1616.
- Lee, J., He, K., Stolc, V., Lee, H., Figueroa, P., Gao, Y., Tongprasit, W., Zhao, H., Lee, I., and Deng, X.W. (2007). Analysis of transcription factor HY5 genomic binding sites revealed its hierarchical role in light regulation of development. *Plant Cell* **19**: 731–749.
- Lewis, D.R., Ramirez, M.V., Miller, N.D., Vallabhaneni, P., Ray, W.K., Helm, R.F., Winkel, B.S.J., and Muday, G.K. (2011). Auxin and ethylene induce flavonol accumulation through distinct transcriptional networks. *Plant Physiol.* **156**: 144–164.
- Leyser, O. (2018). Auxin signaling. *Plant Physiol.* **176**: 465–479.
- Liang, T., Mei, S., Shi, C., Yang, Y., Peng, Y., Ma, L., Wang, F., Li, X., Huang, X., Yin, Y., and Liu, H. (2018). UVR8 interacts with BES1 and BIM1 to regulate transcription and photomorphogenesis in Arabidopsis. *Dev. Cell* **44**: 512–523.
- Liscum, E., and Briggs, W.R. (1995). Mutations in the NPH1 locus of Arabidopsis disrupt the perception of phototropic stimuli. *Plant Cell* **7**: 473–485.
- Liscum, E., and Briggs, W.R. (1996). Mutations of Arabidopsis in potential transduction and response components of the phototropic signaling pathway. *Plant Physiol.* **112**: 291–296.
- Maere, S., Heymans, K., and Kuiper, M. (2005). BiNGO: A Cytoscape plugin to assess overrepresentation of gene ontology categories in biological networks. *Bioinformatics* **21**: 3448–3449.

- Markstädter, C., Queck, I., Baumeister, J., Riederer, M., Schreiber, U., and Bilger, W. (2001). Epidermal transmittance of leaves of *Vicia faba* for UV radiation as determined by two different methods. *Photosynth. Res.* **67**: 17–25.
- Mazza, C.A., and Ballaré, C.L. (2015). Photoreceptors UVR8 and phytochrome B cooperate to optimize plant growth and defense in patchy canopies. *New Phytol.* **207**: 4–9.
- Okushima, Y., et al. (2005). Functional genomic analysis of the AUXIN RESPONSE FACTOR gene family members in *Arabidopsis thaliana*: unique and overlapping functions of ARF7 and ARF19. *Plant Cell* **17**: 444–463.
- Oravecz, A., Baumann, A., Máté, Z., Brzezinska, A., Molinier, J., Oakeley, E.J., Adám, E., Schäfer, E., Nagy, F., and Ulm, R. (2006). CONSTITUTIVELY PHOTOMORPHOGENIC1 is required for the UV-B response in *Arabidopsis*. *Plant Cell* **18**: 1975–1990.
- Peer, W.A., and Murphy, A.S. (2007). Flavonoids and auxin transport: Modulators or regulators? *Trends Plant Sci.* **12**: 556–563.
- Preuten, T., Hohm, T., Bergmann, S., and Fankhauser, C. (2013). Defining the site of light perception and initiation of phototropism in *Arabidopsis*. *Curr. Biol.* **23**: 1934–1938.
- Procko, C., Burko, Y., and Jaillais, Y. (2016). The epidermis coordinates auxin-induced stem growth in response to shade. *Genes Dev.* **30**: 1529–1541.
- Qi, Y., Bai, S., Vogelmann, T.C., and Heisler, G. (2003). Penetration of UVA, UV-B, blue, and red light into leaf tissues of pecan measured by a fiber optic microprobe system. *Proc. of SPIE* **5156**: 281–290.
- Rizzini, L., Favory, J.J., Cloix, C., Faggionato, D., O'Hara, A., Kaiserli, E., Baumeister, R., Schäfer, E., Nagy, F., Jenkins, G.I., and Ulm, R. (2011). Perception of UV-B by the *Arabidopsis* UVR8 protein. *Science* **332**: 103–106.
- Sakai, T., Kagawa, T., Kasahara, M., Swartz, T.E., Christie, J.M., Briggs, W.R., Wada, M., and Okada, K. (2001). *Arabidopsis* nph1 and npl1: Blue light receptors that mediate both phototropism and chloroplast relocation. *Proc. Natl. Acad. Sci. USA* **98**: 6969–6974.
- Santelia, D., Henrichs, S., Vincenzetti, V., Sauer, M., Bigler, L., Klein, M., Bailly, A., Lee, Y., Friml, J., Geisler, M., and Martinoia, E. (2008). Flavonoids redirect PIN-mediated polar auxin fluxes during root gravitropic responses. *J. Biol. Chem.* **283**: 31218–31226.
- Sato, A., Sasaki, S., Matsuzaki, J., and Yamamoto, K.T. (2015). Negative phototropism is seen in *Arabidopsis* inflorescences when auxin signaling is reduced to a minimal level by an Aux/IAA dominant mutation, *axr2*. *Plant Signal. Behav.* **10**: e990838.
- Savaldi-Goldstein, S., Peto, C., and Chory, J. (2007). The epidermis both drives and restricts plant shoot growth. *Nature* **446**: 199–202.
- Schmid, M., Davison, T.S., Henz, S.R., Pape, U.J., Demar, M., Vingron, M., Schölkopf, B., Weigel, D., and Lohmann, J.U. (2005). A gene expression map of *Arabidopsis thaliana* development. *Nat. Genet.* **37**: 501–506.
- Serrano, A.M., Arana, M.V., Vanhaelewyn, L., Ballaré, C.L., Van Der Straeten, D., and Vandenbussche, F. (2018). Following the star: Inflorescence heliotropism. *Environ. Exp. Bot.* **147**: 75–85.
- Seyfried, M., and Fukshansky, L. (1983). Light gradients in plant tissue. *Appl. Opt.* **22**: 1402.
- Shani, E., Weinstain, R., Zhang, Y., Castillejo, C., Kaiserli, E., Chory, J., Tsién, R.Y., and Estelle, M. (2013). Gibberellins accumulate in the elongating endodermal cells of *Arabidopsis* root. *Proc. Natl. Acad. Sci. USA* **110**: 4834–4839.
- Sibout, R., Sukumar, P., Hettiarachchi, C., Holm, M., Muday, G.K., and Hardtke, C.S. (2006). Opposite root growth phenotypes of *hy5* versus *hy5 hyh* mutants correlate with increased constitutive auxin signaling. *PLoS Genet.* **2**: e202.
- Silva-Navas, J., Moreno-Risueno, M.A., Manzano, C., Téllez-Robledo, B., Navarro-Neila, S., Carrasco, V., Pollmann, S., Gallego, F.J., and Del Pozo, J.C. (2016). Flavonols mediate root phototropism and growth through regulation of proliferation-to-differentiation transition. *Plant Cell* **28**: 1372–1387.
- Stanton, M.L., and Galen, C. (1989). Consequences of flower heliotropism for reproduction in an alpine buttercup (*Ranunculus adoneus*). *Oecologia* **78**: 477–485.
- Stracke, R., Favory, J.J., Gruber, H., Bartelniewoehner, L., Bartels, S., Binkert, M., Funk, M., Weisshaar, B., and Ulm, R. (2010b). The *Arabidopsis* bZIP transcription factor HY5 regulates expression of the PFG1/MYB12 gene in response to light and ultraviolet-B radiation. *Plant Cell Environ.* **33**: 88–103.
- Stracke, R., Jahns, O., Keck, M., Tohge, T., Niehaus, K., Fernie, A.R., and Weisshaar, B. (2010a). Analysis of PRODUCTION OF FLAVONOL GLYCOSIDES-dependent flavonol glycoside accumulation in *Arabidopsis thaliana* plants reveals MYB11-, MYB12- and MYB11-independent flavonol glycoside accumulation. *New Phytol.* **188**: 985–1000.
- Tatematsu, K., Kumagai, S., Muto, H., Sato, A., Watahiki, M.K., Harper, R.M., Liscum, E., and Yamamoto, K.T. (2004). MASSUGU2 encodes Aux/IAA19, an auxin-regulated protein that functions together with the transcriptional activator NPH4/ARF7 to regulate differential growth responses of hypocotyl and formation of lateral roots in *Arabidopsis thaliana*. *Plant Cell* **16**: 379–393.
- Tilbrook, K., Arongaus, A.B., Binkert, M., Heijde, M., Yin, R., and Ulm, R. (2013). The UVR8 UV-B photoreceptor: perception, signaling and response. *The Arabidopsis Book* **11**: e0164.
- Timppte, C., Wilson, A.K., and Estelle, M. (1994). The *axr2-1* mutation of *Arabidopsis thaliana* is a gain-of-function mutation that disrupts an early step in auxin response. *Genetics* **138**: 1239–1249.
- Ubeda-Tomás, S., Federici, F., Casimiro, I., Beemster, G.T., Bhalerao, R., Swarup, R., Doerner, P., Haseloff, J., and Bennett, M.J. (2009). Gibberellin signaling in the endodermis controls *Arabidopsis* root meristem size. *Curr. Biol.* **19**: 1194–1199.
- Ulm, R., Baumann, A., Oravecz, A., Máté, Z., Adám, E., Oakeley, E.J., Schäfer, E., and Nagy, F. (2004). Genome-wide analysis of gene expression reveals function of the bZIP transcription factor HY5 in the UV-B response of *Arabidopsis*. *Proc. Natl. Acad. Sci. USA* **101**: 1397–1402.
- Vandenbussche, F., Petrásek, J., Zádňíková, P., Hoyerová, K., Pesek, B., Raz, V., Swarup, R., Bennett, M., Zazimalová, E., Benková, E., and Van Der Straeten, D. (2010). The auxin influx carriers AUX1 and LAX3 are involved in auxin-ethylene interactions during apical hook development in *Arabidopsis thaliana* seedlings. *Development* **137**: 597–606.
- Vandenbussche, F., Tilbrook, K., Fierro, A.C., Marchal, K., Poelman, D., Van Der Straeten, D., and Ulm, R. (2014). Photoreceptor-mediated bending towards UV-B in *Arabidopsis*. *Mol. Plant* **7**: 1041–1052.
- Vanhaelewyn, L., Prinsen, E., Van Der Straeten, D., and Vandenbussche, F. (2016a). Hormone-controlled UV-B responses in plants. *J. Exp. Bot.* **67**: 4469–4482.
- Vanhaelewyn, L., Schumacher, P., Poelman, D., Fankhauser, C., Van Der Straeten, D., and Vandenbussche, F. (2016b). REPRESSOR OF ULTRAVIOLET-B PHOTOMORPHOGENESIS function allows efficient phototropin mediated ultraviolet-B phototropism in etiolated seedlings. *Plant Sci.* **252**: 215–221.
- Vanhaelewyn, L., Bernula, P., Van Der Straeten, D., Vandenbussche, F., and Viczián, A. (2019a). UVR8-dependent reporters reveal spatial characteristics of signal spreading in plant tissues. *Photochem. Photobiol. Sci.* **18**: 1030–1045.

- Vanhaelewyn, L., Van Der Straeten, D., and Vandenbussche, F.** (2019b). Determination of phototropism by UV-B radiation. *Methods Mol. Biol.* **1924**: 131–139.
- Vaseva, I.I., Qudeimat, E. Potuschak, T., Du, Y., Genschik, P., Vandenbussche, F., and Van Der Straeten, D.** (2018). The plant hormone ethylene restricts Arabidopsis growth via the epidermis. *Proc. Natl. Acad. Sci. USA* **115**: E4130–E4139.
- Weller, J.L., Hecht, V., Vander Schoor, J.K., Davidson, S.E., and Ross, J.J.** (2009). Light regulation of gibberellin biosynthesis in pea is mediated through the COP1/HY5 pathway. *Plant Cell* **21**: 800–813.
- Went, F.W.** (1926). On growth accelerating substances in the coleoptile of *Avena sativa*. *Proc. K. Ned. Akad. Wet.* **30**: 10–19.
- Whippo, C.W., and Hangarter, R.P.** (2006). Phototropism: Bending towards enlightenment. *Plant Cell* **18**: 1110–1119.
- Winter, D., Vinegar, B., Nahal, H., Ammar, R., Wilson, G.V., and Provar, N.J.** (2007). An “Electronic Fluorescent Pictograph” browser for exploring and analyzing large-scale biological data sets. *PLoS One* **2**: e718.
- Yin, R., Skvortsova, M.Y., Loubéry, S., and Ulm, R.** (2016). COP1 is required for UV-B-induced nuclear accumulation of the UVR8 photoreceptor. *Proc. Natl. Acad. Sci. USA* **113**: E4415–E4422.
- Zourelidou, M., et al.** (2014). Auxin efflux by PIN-FORMED proteins is activated by two different protein kinases, D6 PROTEIN KINASE and PINOID. *eLife* **3**: e02860.

## Differential UVR8 Signal across the Stem Controls UV-B–Induced Inflorescence Phototropism

Lucas Vanhaelewyn, András Viczián, Els Prinsen, Péter Bernula, Alejandro Miguel Serrano, Maria Veronica Arana, Carlos L. Ballaré, Ferenc Nagy, Dominique Van Der Straeten and Filip Vandebussche  
*Plant Cell* 2019;31;2070-2088; originally published online July 9, 2019;  
DOI 10.1105/tpc.18.00929

This information is current as of November 24, 2019

<b>References</b>	This article cites 106 articles, 49 of which can be accessed free at: <a href="/content/31/9/2070.full.html#ref-list-1">/content/31/9/2070.full.html#ref-list-1</a>
<b>Permissions</b>	<a href="https://www.copyright.com/ccc/openurl.do?sid=pd_hw1532298X&amp;iissn=1532298X&amp;WT.mc_id=pd_hw1532298X">https://www.copyright.com/ccc/openurl.do?sid=pd_hw1532298X&amp;iissn=1532298X&amp;WT.mc_id=pd_hw1532298X</a>
<b>eTOCs</b>	Sign up for eTOCs at: <a href="http://www.plantcell.org/cgi/alerts/ctmain">http://www.plantcell.org/cgi/alerts/ctmain</a>
<b>CiteTrack Alerts</b>	Sign up for CiteTrack Alerts at: <a href="http://www.plantcell.org/cgi/alerts/ctmain">http://www.plantcell.org/cgi/alerts/ctmain</a>
<b>Subscription Information</b>	Subscription Information for <i>The Plant Cell</i> and <i>Plant Physiology</i> is available at: <a href="http://www.aspb.org/publications/subscriptions.cfm">http://www.aspb.org/publications/subscriptions.cfm</a>